NOVA SCHOOL OF SCIENCE & TECHNOLOGY

DEPARTAMENT OF MATERIALS SCIENCE

Catarina Paulino Cidade do Carmo

BSc in Micro and Nanotechnology Engineering

CONTROLLED DRUG DELIVERY FOR SURFACE PROTECTION OF PROSTHESES

MASTER IN MICRO AND NANOTECHNOLOGY ENGINEERING

NOVA University Lisbon

September, 2022

NOVA SCHOOL OF SCIENCE & TECHNOLOGY

DEPARTAMENT OF MATERIAL SCIENCES

Controlled drug delivery for surface protection of prostheses

CATARINA PAULINO CIDADE DO CARMO

BSc in Micro and Nanotechnology Engineering

Adviser: Isabel Maria das Mercês Ferreira
Associate Professor, NOVA University Lisbon SST

Co-advisers: Ana Catarina Bernardino Baptista
Researcher, NOVA University Lisbon SST

Examination Committee:

Chair: João Paulo Miranda Ribeiro Borges,
Associate Professor, NOVA University Lisbon SST

Rapporteurs: Joana Pereira Neto,
Associate Researcher, NOVA University Lisbon SST

Adviser: Isabel Maria das Mercês Ferreira,
Associate Professor, NOVA University Lisbon SST

MASTER IN MICRO AND NANOTECHNOLOGY ENGINEERING

NOVA University Lisbon
September, 2022

Controlled drug delivery for surface protection of prostheses

Para as minhas inspirações, os meus pais.

ACKNOWLEDGMENTS

A realização e conclusão desta dissertação de mestrado não teria sido possível sem a colaboração de várias pessoas, a quem demonstro o meu profundo e sentido agradecimento.

Às minhas orientadoras, Prof. Drª. Isabel Ferreira e Drª. Ana Baptista, por me acompanharem ao longo deste processo, por se mostrarem sempre disponíveis para esclarecer as minhas dúvidas e pelos conhecimentos transmitidos.

Aos meus colegas de laboratório. Miguel, por me guiares, pelo apoio e paciência. Inês, pelo carinho e ensinamentos. O nosso laboratório está cheio de boa gente e por isso agradeço de coração a todos.

À minha parceira de tese. Beatriz, por teres tornado os dias leves, alegres e inesquecíveis. A tese é uma fase marcante das nossas vidas, fui uma sortuda por privar esta fase do teu lado.

Às minhas amigas e colegas de curso. Carol L, Carol V, Bia e Bá, para chegar até aqui percorremos antes 9 semestres, onde os dias foram longos, mas os anos passaram rápido. Obrigada por terem tornado o caminho mais fácil, mas sobretudo, obrigada pela vossa amizade.

A todos os meus amigos que foram capazes de perceber a pouca disponibilidade que por vezes demonstrei e por ouvirem as minhas lamúrias. Para não correr o risco de não mencionar alguém não vou identificá-los, mas farei questão de agradecer pessoalmente a cada um.

À minha família, os mais importantes do meu mundo. Mas principalmente, aos meus pais e ao meu irmão, pelo incentivo e por valorizarem o meu potencial mesmo nos momentos mais difíceis. São vocês que me fazem lutar pelos meus sonhos e é graças a vocês que eles se tornam objetivos e metas.

“Never stop because you are afraid – you are never so likely to be wrong. Never keep a line of retreat: it is a wretched invention. The difficult is what takes a little time; the impossible is what takes a little longer.”

(Fridtjof Nansen)

ABSTRACT

This work aimed to study the application of a multilayer polymeric coating on stainless-steel (SS) surfaces to provide local and controlled drug delivery to prevent the formation of biofilms. The bacteria colonies formed onto non-recognized surfaces placed inside the body could cause serious infections leading to the implant's removal. Therefore, implant's surface functionalization is a key point to overcome this problem.

Using electrospinning and blow-spinning techniques, the SS substrates were coated layer-by-layer with membranes made of cellulose acetate (CA) and polycaprolactone (PCL) fibres containing ibuprofen (Ibu). The fibres retain the mechanical properties of the polymers while also allow for controlled Ibu release in specific locations. As a result, Ibu efficacy improves and the ability of implant rejection decreases. Optical microscopy, scanning electron microscopy, and Raman spectroscopy were used to characterize the fibres.

Following the films production, drug release, swelling, and degradation tests were carried out to simulate in vivo performance of the membranes. Mechanical properties were also evaluated through stress and peeling-off adhesion tests. A layer of chitosan (CHI) was electrosprayed between the substrate and the coating for the peeling-off tests, to evaluate the effect of CHI on adhesion.

Ibu was successfully incorporated into the fibres, but the concentrations and control of its release require further investigation. The electrosprayed CHI layer improved the adhesion of the coating to the surfaces. In conclusion, this research has demonstrated that the films obtained have promising properties for use in the context of implant-related infection treatment.

Keywords: Cellulose acetate, polycaprolactone, ibuprofen, electrospinning, blow-spinning, drug release

RESUMO

Este trabalho teve como objetivo estudar a aplicação de um revestimento polimérico multicamada em superfícies de aço inoxidável (SS) para fornecer libertação local e controlada de fármacos para prevenir a formação de biofilmes. As colónias de bactérias formadas em superfícies não reconhecidas colocadas dentro do corpo podem causar infeções graves que levam à remoção do implante. Portanto, a funcionalização da superfície do implante é um ponto chave para superar este problema.

Utilizando técnicas de eletrofiação e *blow-spinning*, os substratos SS foram revestidos camada por camada com membranas feitas de fibras de acetato de celulose (CA) e de policaprolactona (PCL) incorporando ibuprofeno (Ibu). As fibras retêm as propriedades mecânicas dos polímeros, permitindo também a libertação controlada de Ibu em locais específicos. Como resultado, a eficácia do Ibu melhora e a capacidade de rejeição do implante diminui. Microscopia ótica, microscopia eletrónica de varredura e espectroscopia *Raman* foram utilizadas para caracterizar as fibras.

Após a produção dos filmes, testes de libertação do fármaco, inchamento e degradação foram realizados para simular o desempenho *in vivo* das membranas. As propriedades mecânicas também foram avaliadas por meio de testes de tração e adesão. Uma camada de quitosana (CHI) foi eletropulverizada entre o substrato e o revestimento para avaliar o efeito da CHI nos testes de adesão.

O Ibu foi incorporado com sucesso nas fibras, mas as concentrações e o controlo da sua libertação requerem investigação adicional. A camada de CHI eletropulverizada melhorou a adesão do revestimento às superfícies. Concluindo, esta pesquisa demonstrou que os filmes obtidos possuem propriedades promissoras para uso no contexto do tratamento de infeções relacionadas a implantes.

Palavras chave: Acetato de celulose, policaprolactona, ibuprofeno, eletrofiação, *blow-spinning*, libertação de fármaco

CONTENTS

LIST OF FIGURES

LIST OF TABLES

ACRONYMS

BS	Blow-spinning
CA	Cellulose acetate
CHI	Chitosan
ES	Electrospinning/Electrospray
Ibu	Ibuprofen
MFD	Mean fibre diameter
NSAID	Nonsteroidal anti-inflammatory drug
PCL	Polycaprolactone
SBF	Simulated body fluid
SEM	Scanning electron microscope
SS	Stainless steel

SYMBOLS

A	Absorbance
e	Molar absorption coefficient
c	Molar concentration
l	Optical path
W_0	Original weight
W_d	Dry weight
σ	Stress
ε	Strain
F	Applied force
A_0	Sample area
Δl	Elongation
l_0	Initial length
E	Young's modulus

1

INTRODUCTION

This work aims to investigate multifunctional polymeric coatings containing drug delivery vehicles to prevent the formation of biofilms on implant surfaces. Polymeric coatings must be biocompatible, have good substrate adhesion, and have controlled drug release.

This introduction aims to emphasize the importance of biofilms in the context of implants and to present the approach proposed in this work with the incorporation of the drug in coatings that will serve as an anti-inflammatory agent preventing prosthesis rejections. As a substrate for the coating deposition, stainless steel, a metallic alloy commonly used in biomedical devices, was chosen. These were coated with films made of multilayers of cellulose acetate, polycaprolactone, and chitosan, all of which are well-known biocompatible materials that are frequently used in implant materials. Ibuprofen was chosen as the anti-inflammatory to be loaded into the solutions due to its easy accessibility. Electrospinning, electrospray, and blow-spinning techniques will ensure its ease of production, low cost, and versatility to suit various surface formats.

1.1 Biofilms

Biofilms are microorganism aggregates (bacteria, fungi, protists) that can grow as structured communities on a variety of surfaces while embedded in a polymeric matrix. These biofilms are formed by initially weak links between the bacteria and the surface, which eventually progress to an almost permanent link, followed by the biofilm's own structurization[1].

Bacterial adhesion to implant surfaces occurs primarily through contact with contaminated surfaces, preventing antibiotics and anti-inflammatory drugs from acting as intended. They also become difficult to treat with antimicrobial agents due to the formation of a protective layer around the bacteria. This situation results in recurring or persistent infections, which cause tissue destruction, dysfunction, and implant removal in exchange for a new one, accounting for approximately 15% of all orthopaedic surgeries[2][3].

Figure 1.1 shows the process of biofilm formation from left to right, regardless of infection mechanism: (1) Attachment; (2) Accumulation; (3) Maturation; and (4) Dispersion through the environment[4].

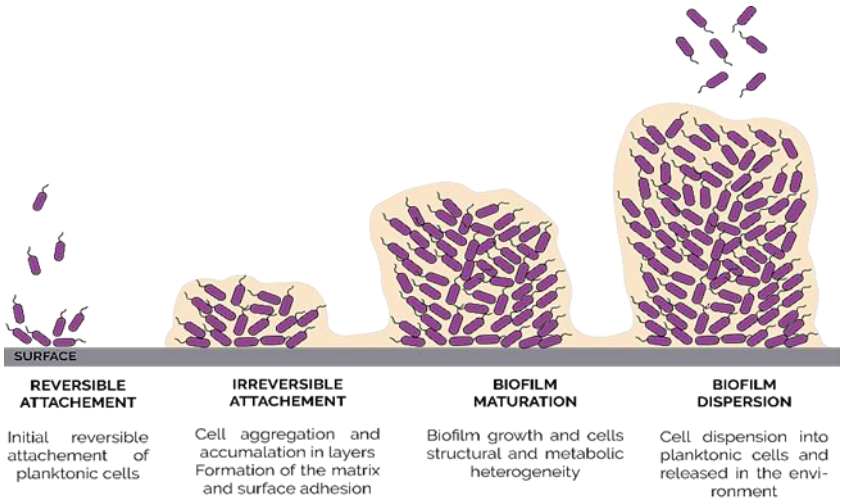

Figure 1.1 – Biofilm formation process. Adapted from [4].

Surface modifications, nanoparticle-based treatments, biocompatible polymer coatings, and antibiotic concentration adjustments are some of the main methods for preventing and combating biofilms[2]. The use of polymer blends as coating materials for controlled drug delivery systems can provide significant benefits, including the ability to easily adjust desired drug release patterns, mechanical properties, and drug release mechanisms, and improved film formation and storage stability[2].

1.2 Implants

Implants are any device or material used to replace or repair a part of the body to improve quality of life or to help re-establish functions lost due to disease or accident. Despite the success of these devices, there is still concern about long-term problems associated with continued exposure of body tissues to implant materials. These concerns stem from the interaction of implant materials with surrounding tissues and physiological fluids[5].

The materials used to make the implants will vary depending on their intended use. The following implantable devices are commonly found in biomedical implants: cardiovascular (stents), neurological (cochlear and retinal), and orthopaedic (bone plates and dental implants)[6].

Metals are by far the most ancient and widely used materials in surgical procedures. This is due to their properties, which include high strength, high fracture resistance, good formability, and, most importantly, biocompatibility, which prevents the body from attacking the implant, resulting in corrosion of the implant, which causes an overall loss of efficiency and can have other negative effects on the body. As a result, stainless steel (SS), titanium and its alloys, cobalt-based alloys, and tantalum are the most used metals in implantable devices[6].

Among metallic implants, SS (especially types 316 and 316L) is a popular choice for orthopaedic surgeries such as fracture fixation and bone plates, owing to its high shear strength when compared to titanium alloys, and the ability to vary corrosion resistance depending on the alloy, making them very versatile, but also because they are inexpensive and simple to handle. As a result, improving the bioactivity and corrosion resistance of SS implants is critical for clinical applications[7].

Major complications with SS implants include allergic reactions to wear debris in the surrounding tissues, corrosion-induced toxicity, and device degradation. Furthermore, previous research has shown that applying protective coatings is one of the most effective ways to protect stainless-steel alloys from corrosion[8].

The following section discusses the technique used in this study to modify 316L SS substrates with a polymer-based sandwich drug release coating.

1.3 Coatings for controlled drug release

After implant placement, controlled drug release coatings are standard procedures used to try to avoid situations such as biofilm formation and associated infections. They are devices that can deliver small but sustained doses of drug to the implantation site while causing minimal systemic toxicity, making drug resistance unlikely in microorganisms[9].

This chapter provides an overview of the drug and the polymers used in the coating of this work.

1.3.1 Polymers

Cellulose acetate (CA) is a cellulose derivative, which is one of the most abundant natural polymers on the planet. It is a biopolymer, which means it is a biodegradable polymer (hydrophilic in nature), biocompatible, nontoxic, and can be functionalized by different groups to achieve the desired properties, making it particularly appealing to researchers[9].

CA solutions are simple to convert into membranes and fibres. These membranes have high chemical and mechanical stability, excellent water affinity, high porosity, and superior transport properties, all of which are desirable properties for tissue engineering scaffolds and drug-delivery devices[9],[10].

Polycaprolactone (PCL) has long been recognized as a biocompatible and biodegradable synthetic polymer. In physiological conditions (such as the human body), PCL is degraded by hydrolysis of its ester linkages and has thus received a lot of attention for use as an implantable biomaterial. It is particularly interesting for the development of long-term implantable devices[11].

PCL membranes form a randomized fibrous and porous matrix that can increase mechanical strength while also allowing for cell proliferation and fluid absorption. However, due to its hydrophobic nature, PCL's use in medicine has been limited. To overcome this disadvantage, PCL has been modified with other biopolymers such as CA to create a hydrophilic property and improve the scaffold's strength and biocompatibility[9]. CA fibres have a high surface area due to their nano size, which increases their ability as drug carriers because the drug is released locally in the target organ or tissue, requiring less drug with fewer side effects[10].

Chitosan (CHI) is a naturally occurring cationic and highly basic linear polymer (polysaccharide) formed by the N-deacetylation of chitin. CHI is made up of units of glucosamine and N-acetyl-D-glucosamine with β (1→4) bonds between them (Figure 1.2 c))[12]. It is ideal for biomedical applications because it is antimicrobial, promotes cell proliferation, is biodegradable, biocompatible, and provides excellent mechanical resistance to biomaterials based on it[13].

CHI can be formed into films, fibres, beads, powders, and solutions. The polymer's cationic nature attracts negatively charged cytokines and growth factors, which is thought to help protect and concentrate cytokines and growth factors secreted by local cells, resulting in accelerated healing[14].

Figure 1.2 shows the chemical structures of CA, PCL, and CHI.

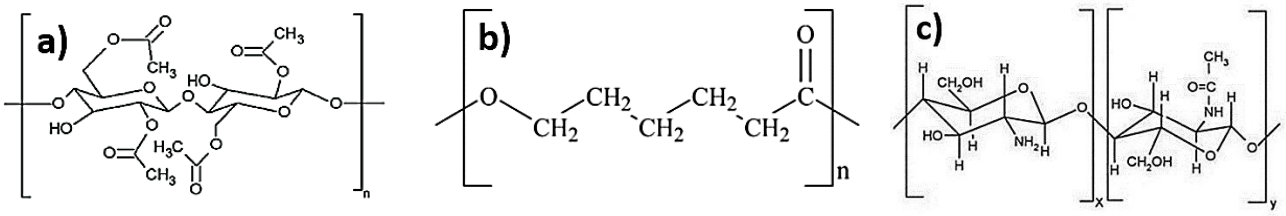

Figure 1.2 - Representation of a) Chemical structure of CA [15], b) Chemical structure of PCL [11], c) Chemical structure of CHI with glucosamine (left) and N-acetyl-D-glucosamine (right) [13].

1.3.2 Ibuprofen

Ibuprofen (Ibu), Figure 1.3, is a popular analgesic-antipyretic-anti-inflammatory medication. Although analgesic usage patterns vary significantly by country, it is likely to rank third behind aspirin and paracetamol in non-prescription over-the-counter use for the relief of symptoms of acute pain, inflammation, and fever. It is also, probably, the least toxic of these three analgesics, with few reports of fatalities from accidental or intentional ingestion or severe adverse reactions[16].

As a nonsteroidal anti-inflammatory drug (NSAID), it focuses on skin applications to treat local pain and inflammation associated with chronic wounds with prolonged inflammation and musculoskeletal problems. When compared to other NSAIDs, the relative topical efficacy of drug reveals that there is a greater flux of Ibu through the skin, indicating that it is suitable for topical administration[17][18]. While other drugs like Ibu appear to be more effective at relieving the symptoms, Ibu compensates by being safer, which is possible due to its short plasma elimination half-life, with little variation from person to person[17].

The use of Ibu in this study aims to confirm drug retention and release of CA and PCL fibres, and not to prevent biofilm formation since it is an anti-inflammatory drug. This choice was made due to their availability and low cost, when compared to antibacterial drugs.

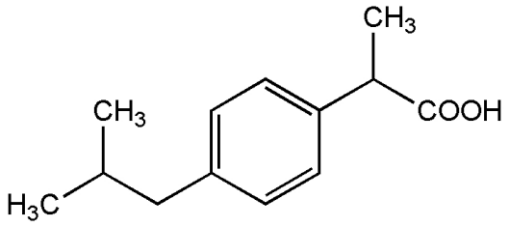

Figure 1.3 - Chemical structure of ibuprofen. Adapted from [16].

1.4 Electrospinning/Electrospray and Blow-spinning membranes

Electrospinning/Electrospray (ES) techniques, Figure 1.4 a), work on the same principles. A syringe containing the solution is placed on a syringe pump and the material inside is extruded with the help of an electrical field applied between the syringe needle and a grounded collector. The physical properties of the polymer solution (viscosity, surface tension) as well as the electrohydrodynamic device parameters influence the final morphology of the obtained polymeric material. When the concentration of the polymer solution is high enough to promote chain entanglements, a polymer jet forms. On the other hand, if the polymer solution concentration is too low, chain entanglements do not form and droplets are sprayed from the needle, resulting in the electrospray process. These techniques were chosen for the fabrication of the membranes due to their

versatility, simplicity, and scalability[19]. They present many process variables that can be used to control the process, such as temperature, humidity, flow, voltage, needle diameter, and distance from the collector to the needle[20].

Blow-spinning (BS) technique, Figure 1.4 b), is a relatively new method for producing polymer micro and nanofibers that is gaining significant interest as a quick, safe, and appealing alternative to the widely used ES. BS employs concentric nozzles, with the polymer solution extruded through the inner nozzle and high-pressure gas released through the outer nozzle. The high-pressure compressed gas causes a polymer solution jet to discharge from the tip of a Taylor cone at the inner nozzle's exit. The jet is then accelerated over the working distance towards the collector. Although the potential for significantly faster fibre production rates and a wider range of available polymer-solvent systems were the primary reasons for choosing the BS method, extensive research is still needed to establish the relationships between the fibrous materials structure and the processing parameters, such as airflow, pistol-target distance, and chamber temperature. The formation of uniform fibres has been shown to be dependent on polymer solution concentration, which influences solution viscosity[21].

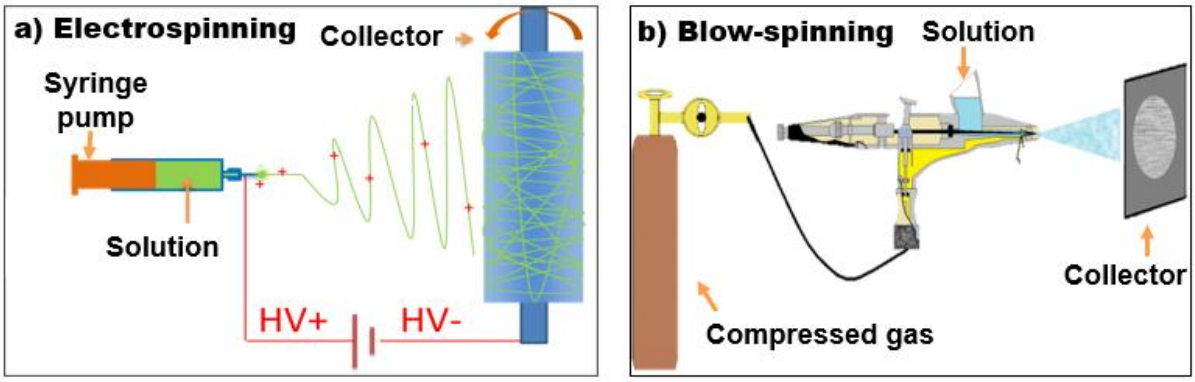

Figure 1.4 - Schematics of a) Electrospinning/Electrospray[22] and b) Blow-spinning[23] setups

Previous studies used Ibu in CA fibres, which were then used to make bandages and wound dressing, to reduce inflammation. The fibres would dissolve quickly, releasing all the Ibu that had been retained in them. This opens the possibility of using fast-dissolving drug delivery for poorly water-soluble drugs like Ibu[24].

Other previous research has shown that CHI coatings can provide corrosive protection for a short period of time due to their fast resorption rate, but their superior biocompatibility and bioactivity can bring additional benefits in terms of biological performance. PCL coatings improved mechanical adhesion to AZ91 alloy substrates (magnesium alloy) and promoted greater spreading and elongation of osteoblastic cells than untreated substrates. Thus, the combination of CHI and PCL into a single coating system has unique properties such as antimicrobialability, osteoinductivity, and strong adhesion to surfaces[25].

Previously[26], our research group investigated the use of dip-coating and ES techniques to prepare alternate layers of CHI and CA fibres containing antibiotics as a protective coating and drug delivery vehicle for metal implants. This thesis will build on those advances by focusing on the ES and BS techniques for encapsulating a model drug (Ibu) into fibres of CA, PCL and CHI deposited on SS substrates. The following objectives were set for this work:

i. Production of CA fibres incorporating Ibu by ES (process optimization).
ii. Production of PCL fibres incorporating Ibu by ES and BS.
iii. Production of a coating with layers of CA and PCL incorporating Ibu.
iv. Evaluation of the obtained drug release profiles.
v. Study of fibres adhesion to SS substrates with a CHI layer on it.

2

MATERIALS AND METHODS

This chapter provides a brief overview of the materials and processes used in this work. Starting with polymeric solution preparation, membrane fabrication, drug release tests, and finally the methods used to analyse and characterize the various membrane properties presented.

2.1 Polymeric solutions

The CA (Sigma-Aldrich, USA, average Mn ~50,000 by GPC, 39.7 wt.% acetyl) solution 12% wt/v, used as solvents dimethylacetamide (≥ 99.8%, Carlo Erba, France) and acetone (≥ 99.5%, Honeywell, Germany), with a ratio of 1:2. The PCL (Sigma-Aldrich, UK, average Mn ~80,000) solution 5% wt/v, used as solvents dichloromethane (Carlo Erba, France) and dimethylformamide (≥ 99.9%, Carlo Erba, France), with a ratio of 7:3. The same quantity of Ibu (Farma-Quimica Sur, Spain), 1 mg, was added to the CA and PCL solutions, resulting in concentrations of about 0.5 g/L.

The CHI (Sigma-Aldrich, USA) solution 0.5% wt/v, used as solvents ultrapure water, and ethanol (≥ 99.8%, Honeywell, Germany), with a ratio of 1:1 and acetic acid (≥ 99.7%, Sigma-Aldrich, USA), 1% v/v.

2.2 Membranes fabrication

The CA membranes were produced using electrospinning technique, the parameters vary according to whether Ibu is incorporated and can be found in Annex A. The PCL membranes were produced using electrospinning or blow-spinning techniques, the parameters can be found in Annex B. The CHI was deposited on SS substrates immediately before the CA or PCL depositions using the electrospray technique, and used the parameters presented in Annex C. Several depositions were performed, resulting in membranes of various configurations.

To obtain only the CA and PCL membranes, depositions were made on aluminium foil, allowed to rest for 24 hours to completely dry, and then removed with a scalpel. The implant material was then represented by depositions on SS substrates (GoodFellow Cambridge Ltd, 316L). The optical microscope (Leica DMi8) confirmed that the SS substrates used had previously[27] been cleaned and mechanically treated (steps presented in Annex D), so it was only necessary to sand and clean them with ethanol as a precaution.

2.3 Drug release tests

A simulated body fluid (SBF) solution was prepared according to a standard protocol [28], at pH 7.4. The constituents of SBF can be found in Annex E. After prepared the SBF solution was then kept in a refrigerator until use.

To conduct the drug release study, an absorption-concentration calibration curve was first created using the following methodology: a solution of SBF-Ibu at a concentration of 20 mg/L was prepared. The SBF-Ibu solution was then diluted sequentially as shown in Annex F, and the absorbance spectra for each concentration were obtained using UV-VIS spectrophotometry (T90+ UV/VIS Spectrometer PG Instruments Ltd).

The drug release from the membranes was studied by immersing each one in 20 mL of SBF solution at 37 ºC and acquiring the absorption spectrum of the SBF solution at regular intervals for subsequent comparison with the calibration curve.

In a previous study[29], an absorption-concentration calibration curve for Millipore water-Ibu was created in the same way as the one already developed. Each membrane was immersed in 20 mL of Millipore water solution at room temperature, and the absorption spectrum of the water was measured at regular intervals for comparison with the calibration curve.

2.4 Characterization

The surface morphology of substrates and coatings was examined using an optical microscope (Leica DMi8) and a scanning electron microscope (SEM Hitachi S2400) with a 20 kV energy beam. Carbon tape was used to fix the samples in the sample holder.

A compositional analysis was performed using Raman spectroscopy (Witec Alpha 300 RAS) to demonstrate the presence of compounds added to the membranes, such as ibuprofen. This device used a monochromatic laser with a wavelength of 532 nm and a power of 1.5 mW to analyse the samples.

CA and PCL membranes were immersed in 20 mL of SBF solution at 37 ºC for swelling studies. After drying with absorbent paper, the samples were initially weighed at 20-minute intervals, and then every 24 hours for 15 days. For degradation studies, CA and PCL membranes were also immersed in 20 mL of SBF solution at 37 ºC. The samples were cleaned in ultrapure water and dried in an oven at 50 ºC until completely dry before being weighed every 24 hours for 15 days.

The stress testing was done by cutting 1x1.5 cm samples, measured the thickness and fixing in a universal mechanical testing machine (Shimadzu AG-50kNG with the “Trapezium2” software). The membranes were stretched at 2 mm/minute by the 1 cm side, with increasing force up to 10 N, until the membrane tore.

The peeling-off tests evaluate the adhesion properties of the polymeric film bonded to SS substrate fixed in a universal mechanical testing machine (Shimadzu AG-50kNG with the “Trapezium2” software). The film was covered with adhesive tape. The SS tip was attached to one of the claws, and the adhesive tape tip was attached to the moving claw, which was pulled at 5 mm/min, with an increasing force up to 5 N, until it detached from the substrate. This procedure was carried out in films made with and without CHI, to evaluate its influence on adhesion.

Figure 2.1 shows the schematics of the overall process considered.

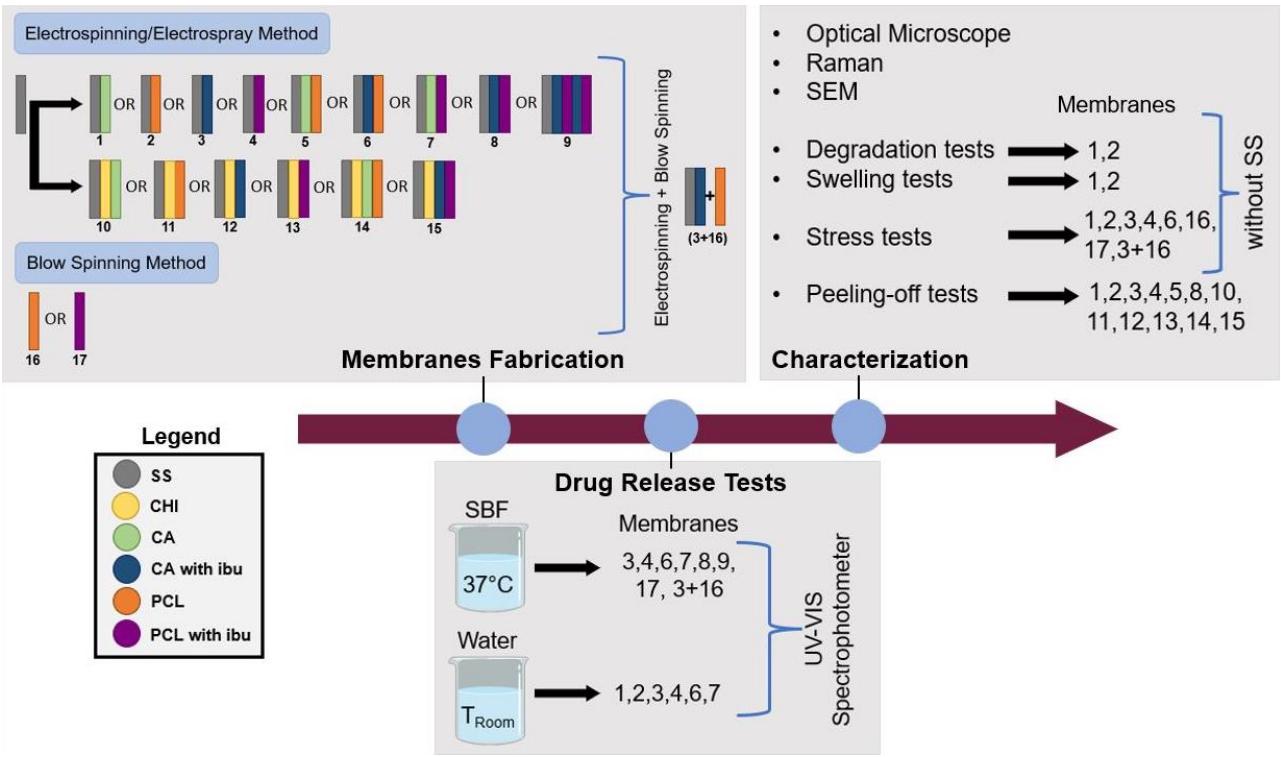

Figure 2.1 - Schematics of the overall process considered

3

RESULTS AND DISCUSSION

The obtained results will be presented and discussed in this chapter. First, the results of the membrane fabrication step will be discussed, specifically the morphology of the fibres obtained with the various conditions and processing solutions, as well as their deposition on SS substrates. Then the drug release tests results and finally the mechanical and degradation membrane tests.

3.1 Membranes fabrication

In this subchapter are presented and described the main fabricated membranes, their morphology and mean fibre diameters (MFD). Membranes were made by electrospinning from four different solutions: 12% wt/v CA, 12% wt/v CA 0.5 g/L Ibu, 5% wt/v PCL, and 5% wt/v PCL 0.5 g/L Ibu. Blow-spinning was also used for some PCL depositions. After deposition the membranes were removed from the aluminium foil and cut into 1.5x1.5 cm squares.

3.1.1 CA membranes

The CA membranes with and without Ibu were produced by the electrospinning technique, using the parameters described in Annex A.

The macroscopic and microscopic images of the obtained CA membrane are shown in Figure 3.1. From the optical microscope image, it is observed that membranes are formed by very thin fibres.

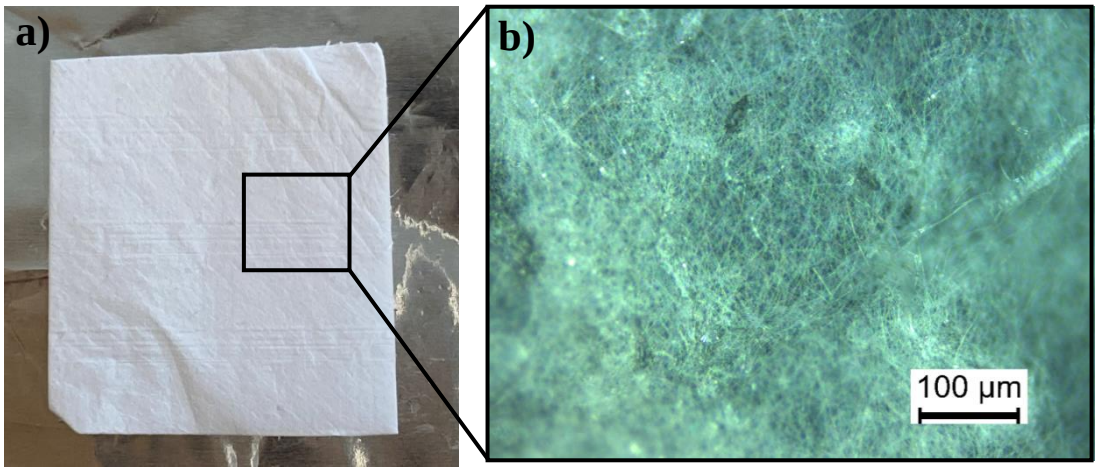

Figure 3.1 - CA membrane with Ibu produced by electrospinning (a) Photograph of the membrane, b) Optical microscope image of the fibres

Figure 3.2 depicts the SEM images of obtained coatings formed by CA fibres without and with Ibu, and MFD is represented in the histogram.

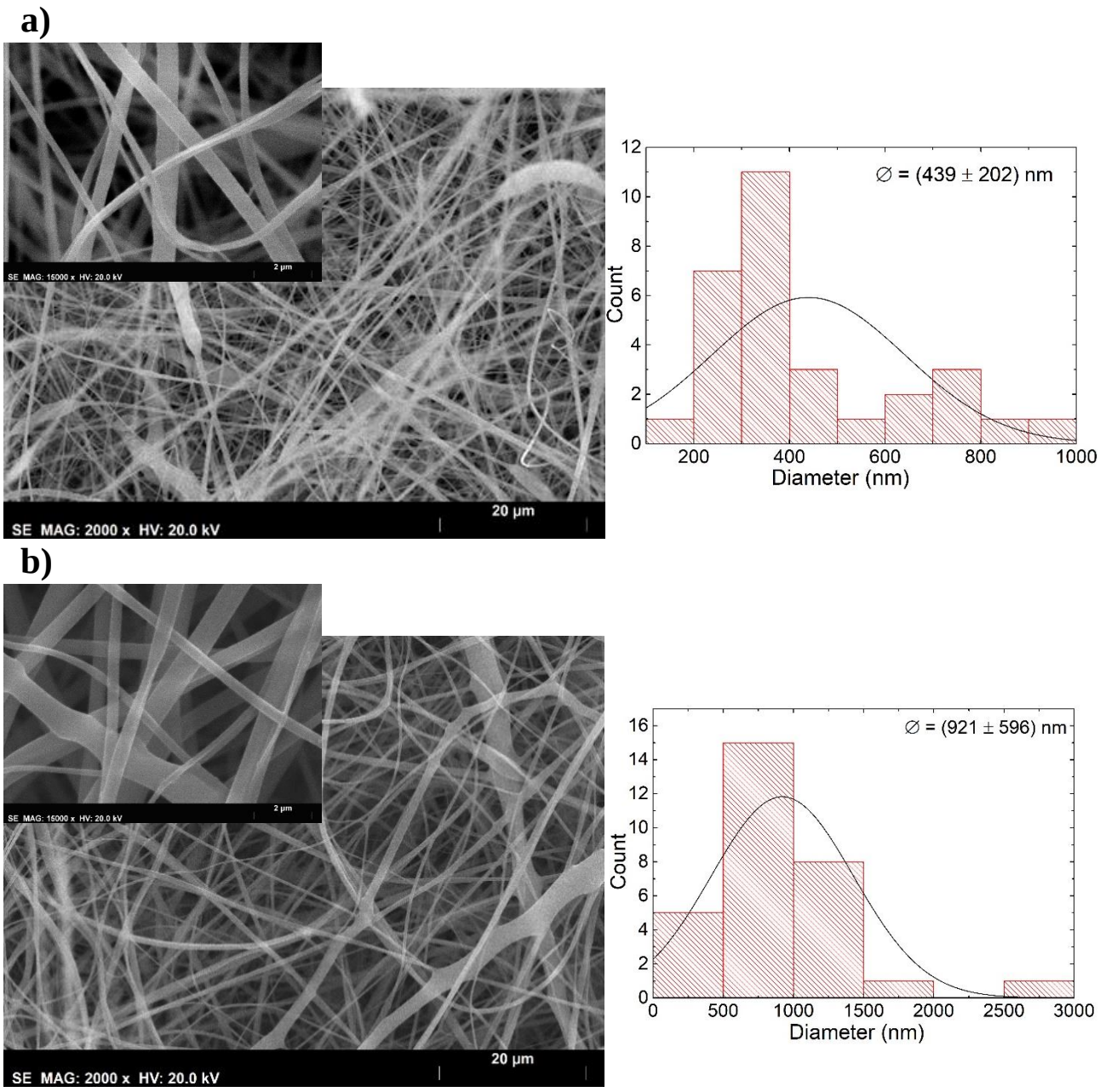

Figure 3.2 - SEM images of CA fibres without Ibu (a) and with Ibu (b), and respective MFD (N=30). Scale bars represent 20 µm or 2 µm in higher magnification images.

Using the ImageJ® program, the average diameters of the fibres were estimated. Comparing the fibres of Figure 3.2 a) and Figure 3.2 b), for the CA membranes without Ibu, the MFD is 439 ± 202 nm, and for the CA membranes with Ibu the MFD is 921 ± 596 nm. The mean diameter and its variance are larger for CA Ibu fibres. This difference can be explained by an increase in solution viscosity when Ibu is added, resulting in the production of fibres with an overall larger diameter when compared to CA electrospun fibres without Ibu. However, due to the small amount of Ibu in the solution, it is possible that not all fibres contain Ibu, resulting in a larger variation in diameters.

3.1.2 PCL membranes

The PCL membranes with and without Ibu, were mostly produced by electrospinning, and some by blow-spinning. The electrospinning parameters used can be found on Annex B.

Figure 3.3 depicts the SEM images of obtained coatings formed by PCL fibres without and with Ibu produced by electrospinning, and MFD is represented in the histogram.

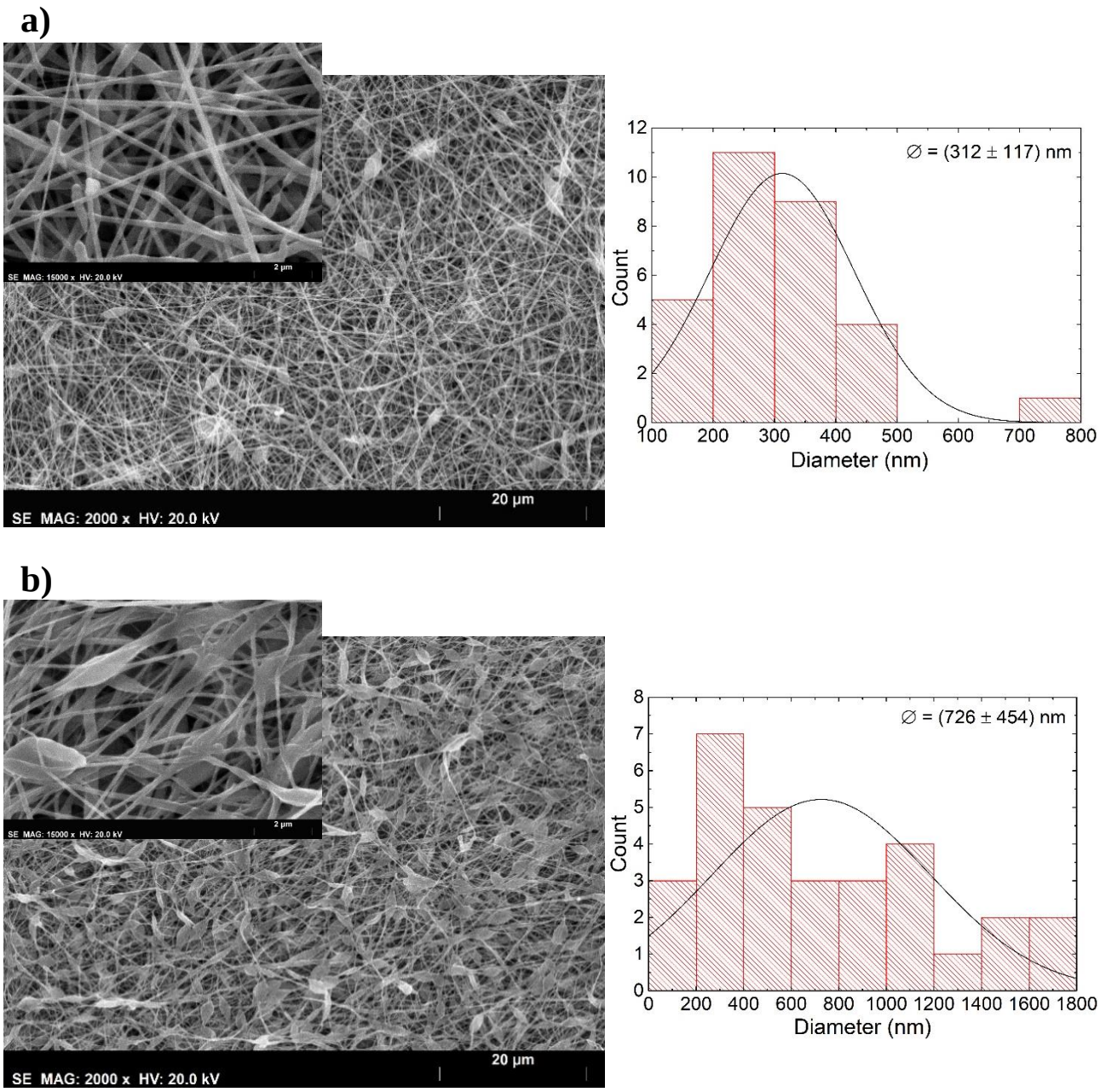

Figure 3.3- SEM images of PCL fibres without Ibu (a) and with Ibu (b), and respective MFD (N=30). Scale bars represent 20 µm or 2 µm in higher magnification images.

Comparing the images of Figure 3.3 a) and Figure 3.3 b), the difference in fibres morphology is clear. For the PCL membranes without Ibu, the MFD is 312 ± 117 nm, and for the PCL membranes with Ibu the MFD is 726 ± 454 nm. As well as CA membranes, the difference in diameters and morphology can be explained by an increase in solution viscosity when Ibu is added, resulting in the production of fibres with a larger diameter when compared to PCL electrospun fibres without Ibu. Fibres from membranes with Ibu also show wider zones, although it is not possible to conclude whether Ibu is accumulated there or whether the increased viscosity of the PCL and Ibu solution is promoting these tangles and/or fibre fusion.

3.1.3 CA and PCL membranes

Double sequential CA and PCL layer membranes were formed with and without Ibu. First CA by electrospinning followed by electrospinning or blow-spinning PCL. The electrospinning parameters can be found on Annex A, and Annex B, respectively.

Figure 3.4 depicts the SEM images of those membrane coatings without and with Ibu produced by electrospinning, MFD histogram is shown next to respective SEM image.

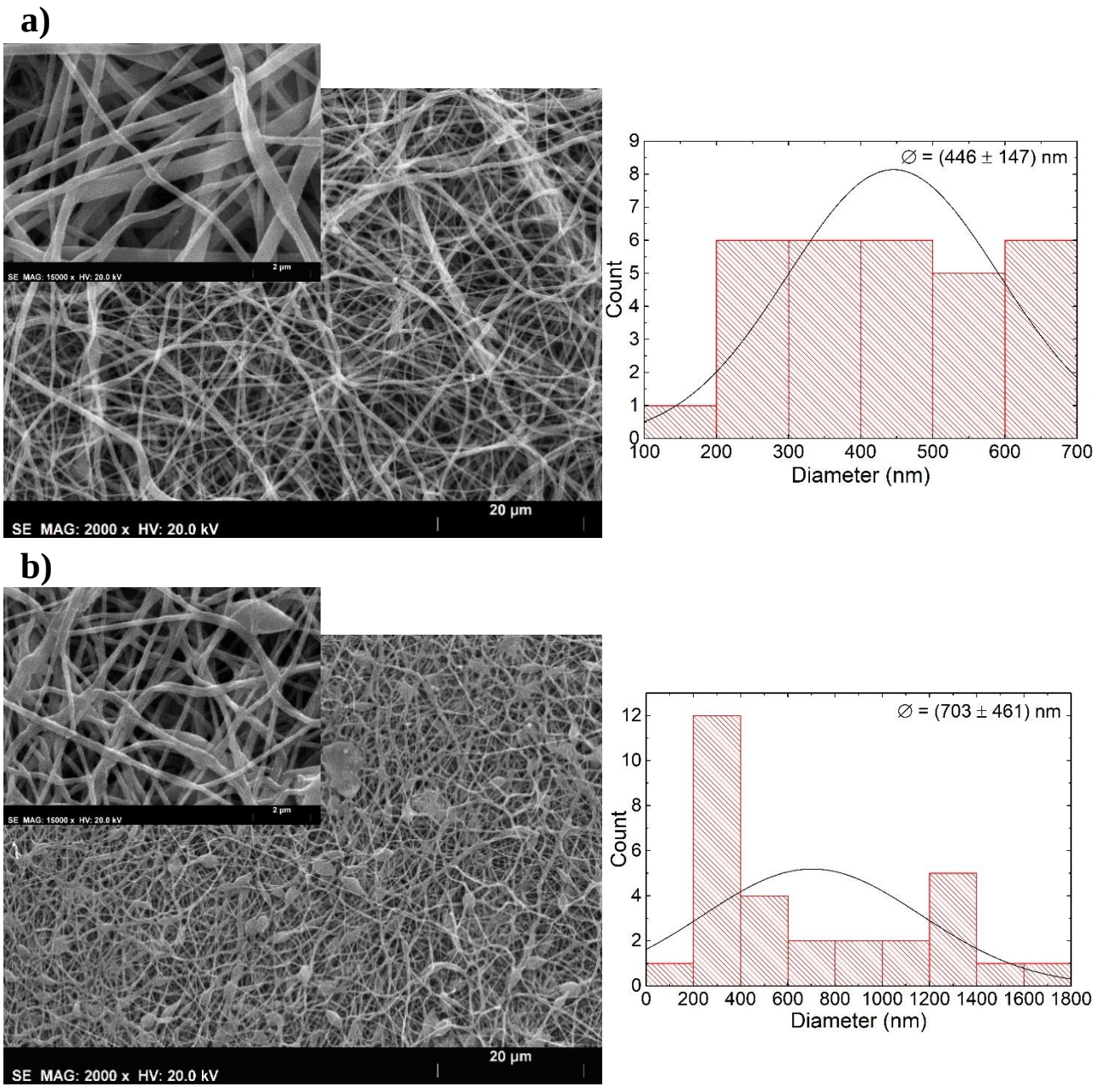

Figure 3.4 - SEM images of CA and PCL fibres without Ibu (a) and with Ibu (b), and respective MFD (N=30). Scale bars represent 20 µm or 2 µm in higher magnification images.

Comparing the fibres of Figure 3.4 a) and Figure 3.4 b), their morphology is comparable to the SEM of PCL fibres without and with Ibu of Figure 3.3 a) and Figure 3.3 b). For the CA and PCL membranes without Ibu, the MFD is 446 ± 147 nm, and for the CA and PCL membranes with Ibu the MFD is 703 ± 461 nm, which is also in the same range of the MFD for PCL fibres. Since PCL is the top layer, it would be the one observed in the SEM images, top view, if there was no fusion with the previous CA layer during deposition.

3.2 Coatings in SS substrates

Medical grade SS substrates were used to simulate prostheses surface. The CA and PCL layers depositions were carried out in a similar way as the previous ones in the aluminium foil. The SS substrates used for coatings should first be treated with mechanical and/or chemical abrasion to remove surface oxides and create anchor sites for the film/membranes fix and adhere.

The SS substrates used had already been treated by a student who had done a similar study the previous year[27], the steps can be found on Annex D. Observing the SS substrates using an optical microscope (Figure 3.5), that was confirmed. It was only necessary, as a precaution, to sand and then clean them with ethanol.

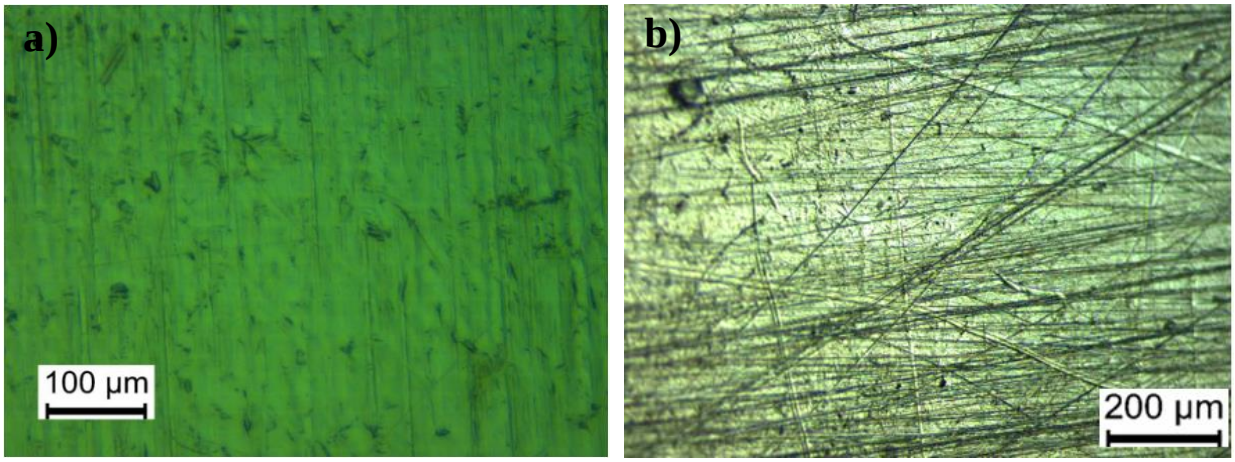

Figure 3.5 - Optical microscope image of stainless-steel substrate a) before treatment[27] and b) after treatment

The CA, PCL and CHI solutions were deposited by ES in SS substrates connected with aluminium adhesive tape to an aluminium foil-coated target, as shown in the experimental setup of the Figure 3.6. This setup has a copper ring attached to the syringe needle, that contains the solution, to collimate the flow and to decrease fibre dispersion to the edges of the SS substrates. As the setup starts operating, the fibres would begin to deposit slowly on the substrate, with random orientation, producing a membrane. The deposition parameters used for the CA, PCL, and CHI solutions are referred in Annex A, Annex B, and Annex C, respectively. As previously reported[27], the CHI layer was introduced to enhance the adhesion of the CA membranes to the SS substrates, it will not intervene in the drug release process.

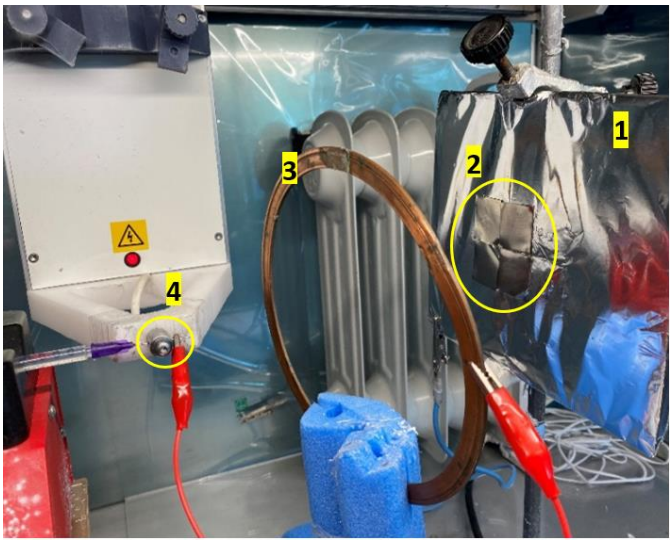

Figure 3.6 - Experimental setup of electrospinning/electrospray collector (1) with four SS substrates (2) attached to it and copper ring (3) attached to the syringe needle (4) by crocodiles.

3.3 Drug Release

To determine the exact quantity of Ibu present in the total membrane, the solutions containing Ibu were completely used to produce the membranes. The membranes were then cut in approximately 10% of the total membrane. However, the quantity of Ibu in these membranes could not be accurately quantified because they were not uniform, with the middle part of the total membrane being thicker and thus more concentrated than the rest. In addition to the membrane waste that could not always be removed from the aluminium foil.

3.3.1 In SBF

To obtain the calibration curve of Ibu in SBF, an SBF-Ibu solution with a concentration of 20 mg/L was prepared, dilutions were made to obtain different concentrations in intervals of 1 mg/L, from 0 mg/L to 20 mg/L. The absorption spectra for the different concentrations are shown in Figure G.1 in Annex G.

The calibration curve of Figure 3.7 is obtained by the maximum absorption value of the peak at 222 nm and 211 nm. Equation (3.1) relates the absorption and concentration obtained from the linear regression of calibration curve of peak of 222 nm and Equation (3.2) is obtained from the peak of 211 nm. Thus, is possible to estimate the concentration when the absorbance is known.

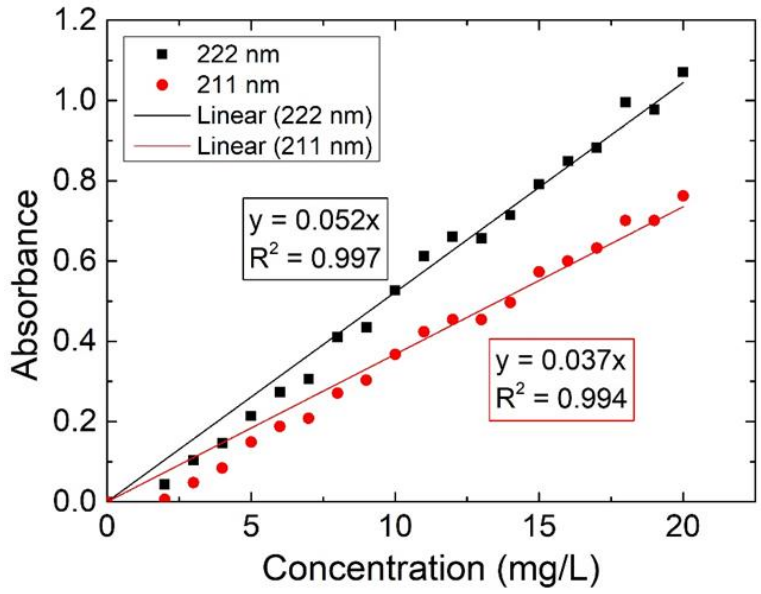

Figure 3.7 - Absorption spectra for the different ibuprofen concentrations on SBF and calibration curve of the two obtained peaks

From the calibration curve was obtained the following empirical correlation between absorption and Ibu concentration in SBF.

$$\text{Concentration ibu 222 nm}\left(\frac{\text{mg}}{\text{L}}\right) = \frac{\text{ABS}}{0.052} \tag{3.1}$$

$$\text{Concentration ibu 211 nm}\left(\frac{\text{mg}}{\text{L}}\right) = \frac{\text{ABS}}{0.037} \tag{3.2}$$

The Beer-Lambert law states that the molar concentration (c) and the absorbance (A) of a solution have a direct proportionality, represented by the Equation (3.3). A notice to justify the deviation of this low to lower concentrations which is due to the sensibility limitations of the equipment used.

$$A = e\ (\mathrm{M^{-1}.cm^{-1}}) \times c\ (\mathrm{M}) \times l\ (\mathrm{cm}) \tag{3.3}$$

Drug release tests were performed by measuring the absorption spectrum of SBF medium were CA and/or PCL membranes with Ibu were immersed, at certain intervals, until the end of 7 days. The obtained spectra are shown in Figure H.1, Figure H.2, Figure H.3, Figure H.4, Figure H.5, Figure H.6 and Figure H.7 in Annex H.

Figure 3.8 shows the average variation of drug release concentration with time of all different membranes in SBF, that was obtained using Equation (3.2), due to the similar absorbance peaks in 211 nm.

To estimate the quantity of Ibu released to the SBF medium, the final values of concentration obtained for every membrane are multiplied by the 20 mL of SBF used. The final values of released Ibu are presented in Table 3.1.

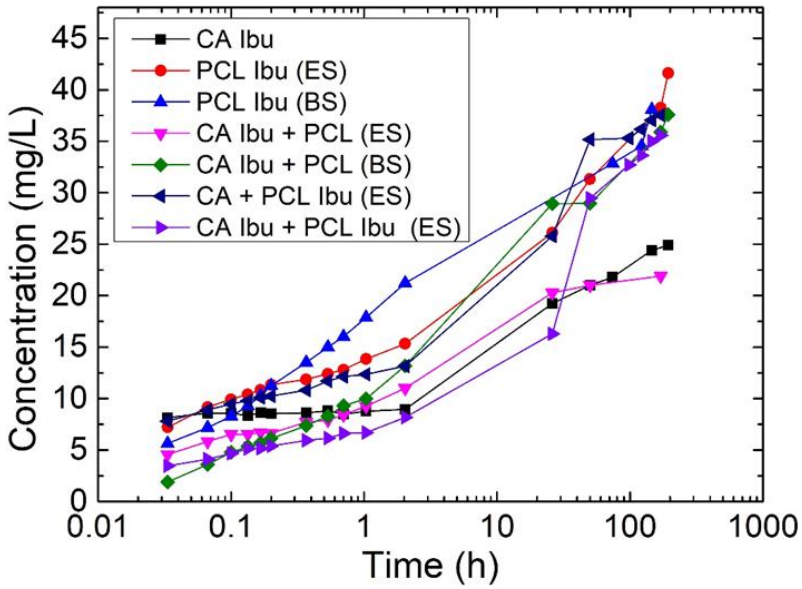

Figure 3.8 - Average variation of drug release concentration with time in SBF.

Table 3.1 – Estimated final quantity of Ibu released in SBF from each membrane after 190h

Membrane	Ibu released (mg)
CA Ibu	0.498
PCL Ibu (ES)	0.832
PCL Ibu (BS)	0.762
CA Ibu + PCL (ES)	0.438
CA Ibu + PCL (BS)	0.789
CA + PCL Ibu (ES)	0.779
CA Ibu + PCL Ibu (ES)	0.700

Figure 3.8 compares various membrane behaviours in drug release. Starting with **PCL Ibu (ES)** and **PCL Ibu (BS)**, the BS membrane allows for faster drug release at the beginning due to its greater porosity, but at the end it becomes very similar. The PCL-BS membrane shows a linear release over time while for PCL-ES it shows a smaller variation up to 2h and then the release is as well faster. Due to porosities the PCL dissolution is faster in BS membranes while in ES it needs more time to start dissolve PCL and then release the drug.

Comparing **CA Ibu + PCL (ES)** to **CA Ibu + PCL (BS)**, it follows the same trend as the isolated PCL membranes, indicating that the BS-fabricated membrane allows for greater drug release due to their porosity, whereas the ES-fabricated membrane acts as a retarding layer.

Comparing **CA Ibu + PCL (ES)** to **CA + PCL Ibu (ES**), their behaviour is very similar up to 20 h. Following that, the membrane with Ibu incorporated into the PCL membrane releases drug more easily than when incorporated into the CA membrane.

The **CA Ibu + PCL Ibu (ES**) layers behave similarly to the **CA + PCL Ibu (ES**) layers. However, the concentration is lower, and should be higher since both layers contain Ibu. This effect is caused by a possible difference in the drug content incorporated into the membranes due to the non-radial uniformity of the thickness of the layers.

The values in the Table 3.1 are inaccurate due to the non-uniform distribution of Ibu in the membrane. To obtain more precise results, it would be necessary, for example, to increase the number of samples or to use a more specific technique for Ibu quantification, as the absorption of SBF salts or polymers can hide the Ibu absorption values.

3.3.2 In water

In a previous work[29], the calibration curve of Ibu in water was obtained in a similar way to in SBF. A 20 mg/L water solution was prepared, and dilutions were made to obtain different concentrations in 1 mg/L intervals ranging from 0 mg/L to 20 mg/L. The 222 nm peak is the most cited in the literature, so it was the value chosen to construct the graph of the calibration curve. The empirical correlation between absorption and Ibu concentration in water is shown in the Equation (3.4), provided by the calibration curve[29].

$$\text{Concentration ibu 222 nm}\left(\frac{\text{mg}}{\text{L}}\right) = \frac{\text{ABS}}{0.0378} \tag{3.4}$$

Drug release tests were performed by measuring the absorption spectrum of water medium were all CA and/or PCL membranes with Ibu were immersed, at certain intervals, until the end of 7 days. The obtained spectra are shown in Figure H.8, Figure H.9, Figure H.10, Figure H.11 and in Annex H. The average variation of concentration with time of all different membranes was obtained using the corresponding absorption peak at 222 nm and Equation (3.4).

Figure 3.9 shows the average variation of drug release concentration with time of all different membranes in water, that was obtained using Equation (3.4), due to the similar absorbance peaks in 222 nm.

To estimate the quantity of Ibu released to the water medium, the final values of concentration obtained for every membrane are multiplied by the 20 mL of water used. The final values of released Ibu are presented in Table 3.2.

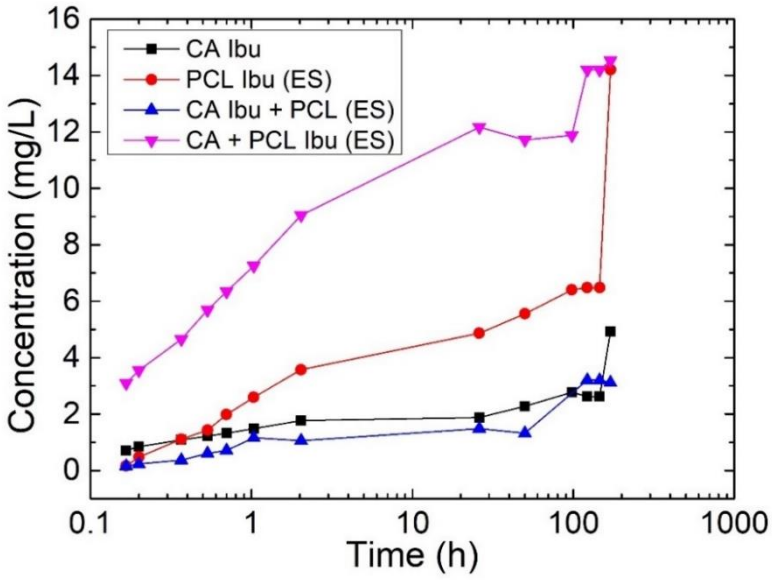

Figure 3.9 - Average variation of drug release concentration with time in water.

Table 3.2 – Estimated final quantity of Ibu released in water from each membrane after 190h

Membrane	Ibu released (mg)
CA Ibu	0.098
PCL Ibu (ES)	0.284
CA Ibu + PCL (ES)	0.062
CA + PCL Ibu (ES)	0.290

Figure 3.9 shows that the **CA Ibu** and **CA Ibu + PCL** membranes behave very similarly, releasing a low amount of drug up to 100 hours. After that, it seems that the tendency is for the release to be greater in the CA Ibu membranes, suggesting that the PCL is retaining the drug in the CA Ibu + PCL (ES) membrane. However, to be conclusive, the study should have been conducted over a longer period of time and with more samples.

When the release of **PCL Ibu** membrane is compared to the release of **CA + PCL Ibu** membrane, it appears that the junction of CA + PCL Ibu has a higher initial drug release in the first 10 h, whereas PCL Ibu has a more controlled release initially, then firing at around 180 h for ending with equal drug releases.

According to this graph, drug release is faster when PCL Ibu is on top of the CA membrane. At least two reasons may cause this behaviour. One is the fact that when placed on top of the CA membrane the PCL Ibu is more porous, which increases drug release, the second is the fact that the PCL Ibu membrane that was deposited on top of the CA membrane contains more drug than the single PCL Ibu membrane. To understand the difference, more results would be needed to have sufficient statistics.

The values in the Table 3.2 are inaccurate due to the non-uniform distribution of Ibu in the membrane. To obtain more precise results, it would be necessary, for example, to increase the number of samples or to use a more specific technique for Ibu quantification, as the absorption of polymers can hide the Ibu absorption values.

3.3.3 Compositional and morphological analysis

To identify the presence of Ibu in CA and PCL membranes, 5 samples (CA, PCL, Ibu, CA Ibu, PCL Ibu) were prepared for analysis in the Raman spectrometer. Figure 3.10 a) shows the obtained spectra for CA and CA Ibu membranes, while Figure 3.10 b) shows the obtained spectra for PCL and PCL Ibu membranes and Figure 3.10 c) shows the obtained spectra for Ibu.

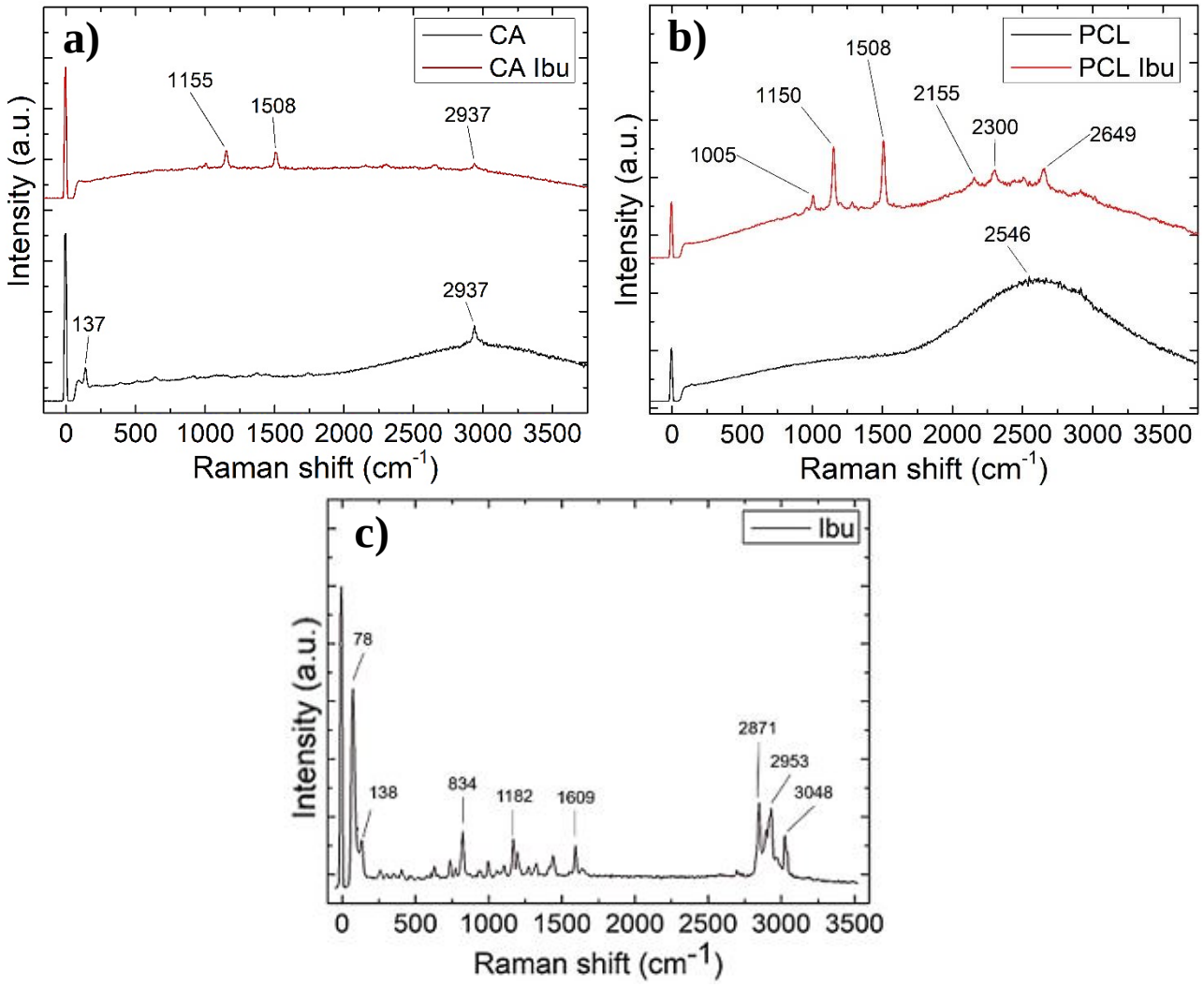

Figure 3.10 - Raman spectra of a) CA membranes with and without Ibu, b) PCL membranes with and without Ibu and c) Ibu

Although the obtained spectra differ in terms of shape or in a small displacement, as is natural since they are different membranes, characteristic peaks of the CA, PCL and Ibu are observed in Figure 3.10 a) and Figure 3.10 b). The 1155 cm^{-1} and 1508 cm^{-1} peaks were found in CA Ibu membranes, while 1150 cm^{-1} and 1508 cm^{-1} were found in PCL Ibu membranes, corresponding to Ibu's characteristic peaks 1182 cm^{-1} and 1609 cm^{-1}, since these are not represented on the isolated spectra of CA and PCL membranes.

Thus, it can be said that the presence of Ibu in CA and PCL membranes was confirmed by Raman spectroscopy, guaranteeing the produced fibres contain Ibu.

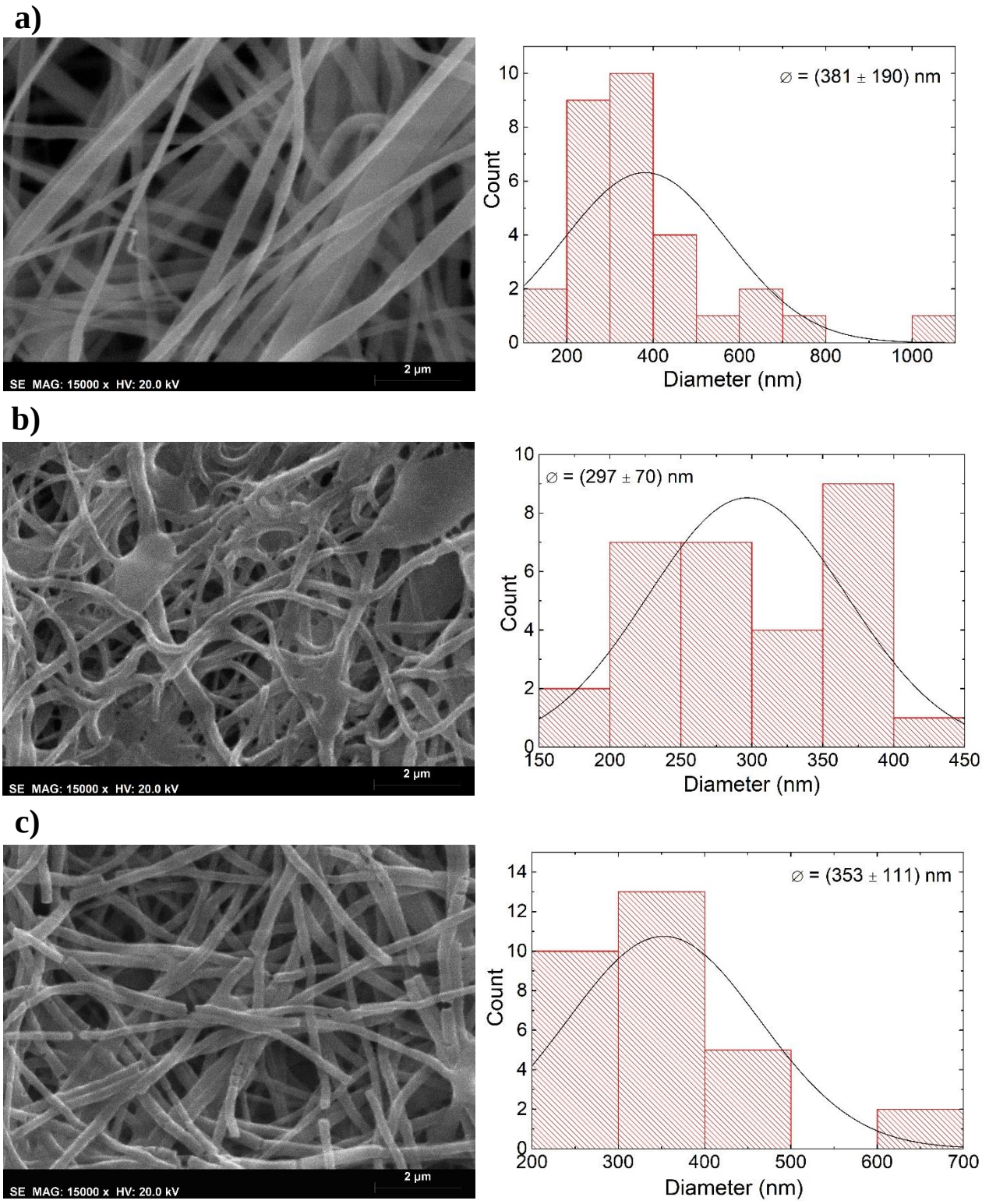

Figure 3.11 - SEM images of membranes after 190 hours of drug release a) CA Ibu, b) PCL Ibu, c) CA + PCL Ibu, and respective MFD (N=30). Scale bars represent 2 µm.

After drug release the MFD for the CA Ibu membranes is 381 ± 190 nm, for the PCL Ibu is 297 ± 70 nm and for CA+PCL Ibu is 353 ± 111 nm. Comparing these results with the ones from sub-chapter 3.1, there is a general decrease in MFD, which is significantly lower than the corresponding membranes before release and slightly lower than the membranes without Ibu, indicating that both Ibu and CA and PCL polymers were released during the drug release process.

3.4 Mechanical and degradation tests of membranes

The degradation, swelling, stress, and peeling-off tests are all covered in this chapter. The degradation tests revealed how long it would take for the degradation to begin and when it would become noticeable. Swelling tests were performed in this chapter to determine how the fibre membrane expanded when immersed in SBF solution and to forecast how it would react in the human body. The stress tests were performed to ensure that the fibre membrane could withstand some tearing. Finally, peeling-off tests were performed to assess membrane adhesion to the substrate and the influence of the CHI layer.

3.4.1 Degradation tests

During the immersion of membrane in medium water or SBF the CA and PCL fibers tend to swell and possibly loss mass. As mass loss is a direct measurement to quantify polymer degradation, degradation tests were performed by weighing the membranes and placing them in SBF solution at 37ºC, to simulate body temperature. Before weighing the membranes, they were washed in Millipore water and placed in the oven at 50 ºC until completely dry. This process was repeated at 24-hour intervals for 15 days. The mass loss of the replicas was calculated according to the Equation (3.5), where W_0 is the original weight of each sample before degradation, and W_d is the dry weight, after the degradation.

$$Mass\ loss\ (\%) = \frac{W_0 - W_d}{W_0} \times 100 \tag{3.5}$$

Figure 3.12 shows the plots of the mass loss vs time of the CA and PCL membranes, obtained to access the mass loss rates observed for both polymers. The most significant loss of mass in the case of CA was 15% at the end of 48 hours. However, this value was never exceeded, and the mass loss stabilized between 5% and 10% after 10 days. The mass loss was relatively low throughout the process, so the degradation is primarily due to measurement reproducibility. In the case of PCL, there is a significant loss of mass of 27% after 48 hours, which returns to this value after 10 days and stabilizes at 30% after 13 days. The larger variations in mass midway through the process can be attributed to the cleaning and drying process. Since PCL is hydrophobic and semicrystalline, its degradation is relatively slow 2-4 years. However recent studies of the degradation of PCL of electrospun fibres shows a mass loss of about 30% in 15 days and 100% loss in 60% when in phosphate buffered saline (PBS) medium[30]. Due to high surface area of fibres may hinder the water penetration inside the nanofibers, so water absorption occurs faster, resulting in a fast degradation rate[31]. To complement this information sweeling tests were also performed.

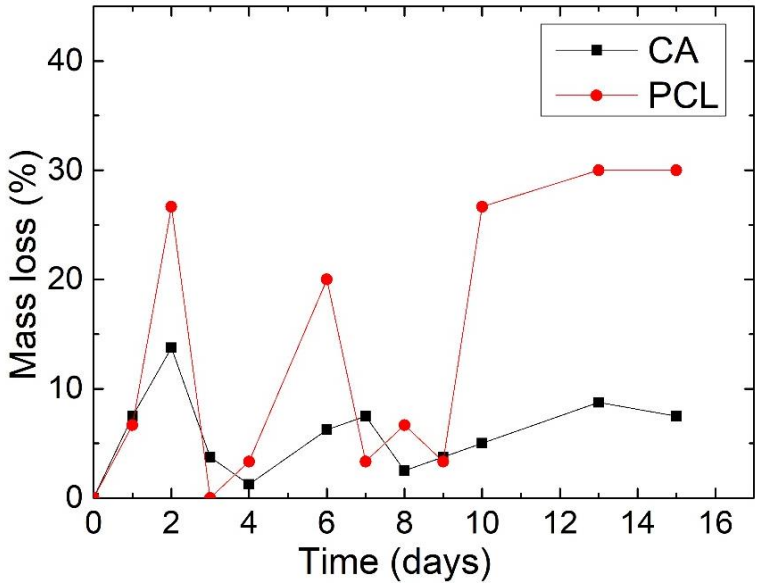

Figure 3.12 - Average percentage of mass loss of the CA and PCL membranes in the degradation process when submerged in SBF (membranes without Ibu)

3.4.2 Swelling tests

Swelling tests were performed by weighing the membranes and placing them in SBF solution at 37ºC, to simulate body temperature. Before weighing the membranes, they were dried with absorbent paper. This process was initially repeated 6 times for periods of 20 minutes and then, 24-hour intervals for 15 days. The swelling ratio was calculated according to Equation (3.6), where W_0 is the original weight of each sample before swelling, and W_d is the dry weight, after the swelling process.

$$Swelling\ Ratio\ (\%) = \frac{W_d}{W_0} \times 100 \tag{3.6}$$

Figure 3.13 depicts the sweeling results for CA and PCL membranes. The CA membrane results show a rapid increase, which corresponds to a maximum swelling of 379% after 1 hour. The sweeling ratio decreases with increasing swelling time, which is likely related to the drying method and possible loss mass of the membranes when dried. The results for PCL membranes show a very low swelling ratio throughout the process, peaking at 213% after 6 days and then stabilising between 115% and 135%. The low swelling ratio is expected because PCL is reported to be hydrophobic, which means it is insoluble in any type of aqueous solution[31], however for membranes formed by fibres the sweeling is usually higher as explained previously for mass loss. Furthermore, some studies[30] also reported that swelling can range between 200-300%. Therefore, this swelling and mass losses explain the high drug delivery in PCL Ibu membranes. Concerning CA membranes, the mass loss is low while the swelling is very high, which is a good characteristic for drug carriers. However, when needed drug retention PCL can be a choice.

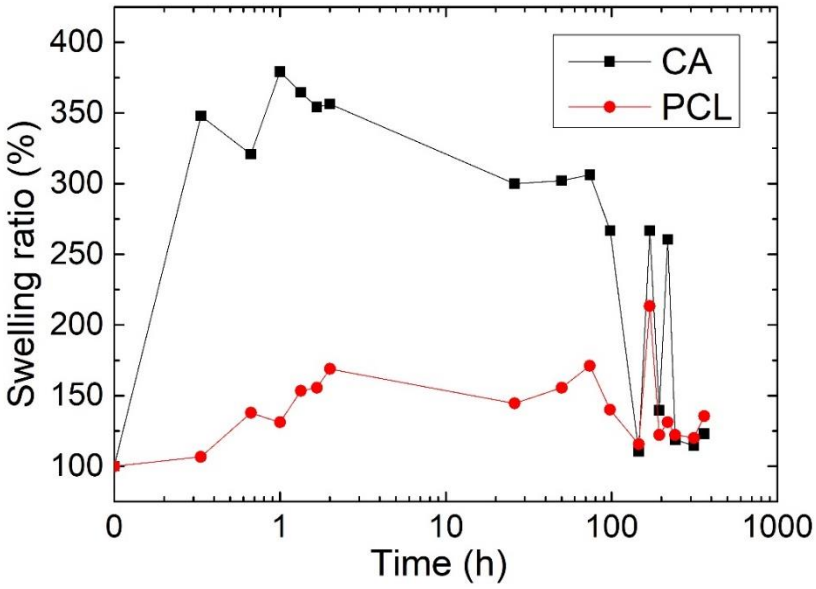

Figure 3.13 - Average percentage change in the mass of CA and PCL membranes in the swelling process when submerged in SBF (membranes without Ibu).

3.4.3 Stress tests

Stress tests were done in 1x1.5 cm membranes, using a universal mechanical testing machine that would, at 2 mm/minute, push the 1 cm side of the membrane, with increasing force up to 10 N, until the membrane tore. The Figure 3.14 a) shows the experimental setup of the membrane in the machine.

The stress tests were performed to obtain the maximum stress (σ) and strain (ε) of the membranes. The Figure 3.14 b) shows an example of a stress-strain curve[32].

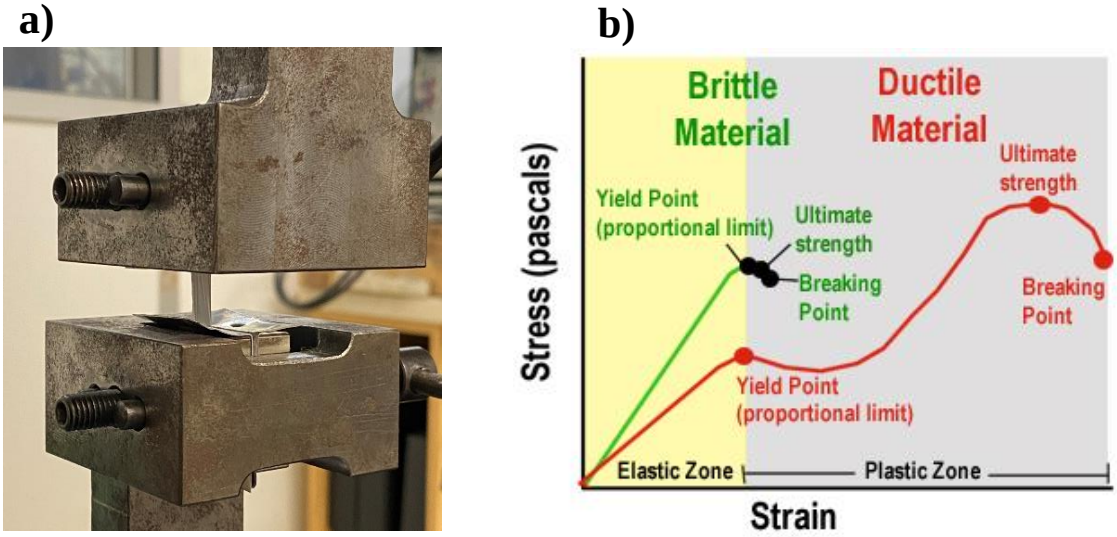

Figure 3.14 - a) Membrane in the mechanical test machine, b) Typical stress-strain curve for brittle and ductile materials[32].

The stress (σ) is the ratio between the applied force (F) and the sample area (A), represented by the Equation (3.7) The strain (ε) is the ratio between the elongation (Δl) of the samples and their initial length (l_0), represented by the Equation (3.8).Young's modulus is the relation between strength and elongation, i.e., the slope in the linear region of the curve, represented by the Equation (3.9).

$$\sigma\ (Pa) = \frac{F\ (N)}{A\ (m^2)} \tag{3.7}$$

$$\varepsilon = \frac{\Delta l\ (mm)}{l_0\ (mm)} \tag{3.8}$$

$$E\ (Pa) = \frac{\sigma\ (Pa)}{\varepsilon} \tag{3.9}$$

Figure 3.15 show the stress-strain curves for a sample of each type of membrane used in the tests.

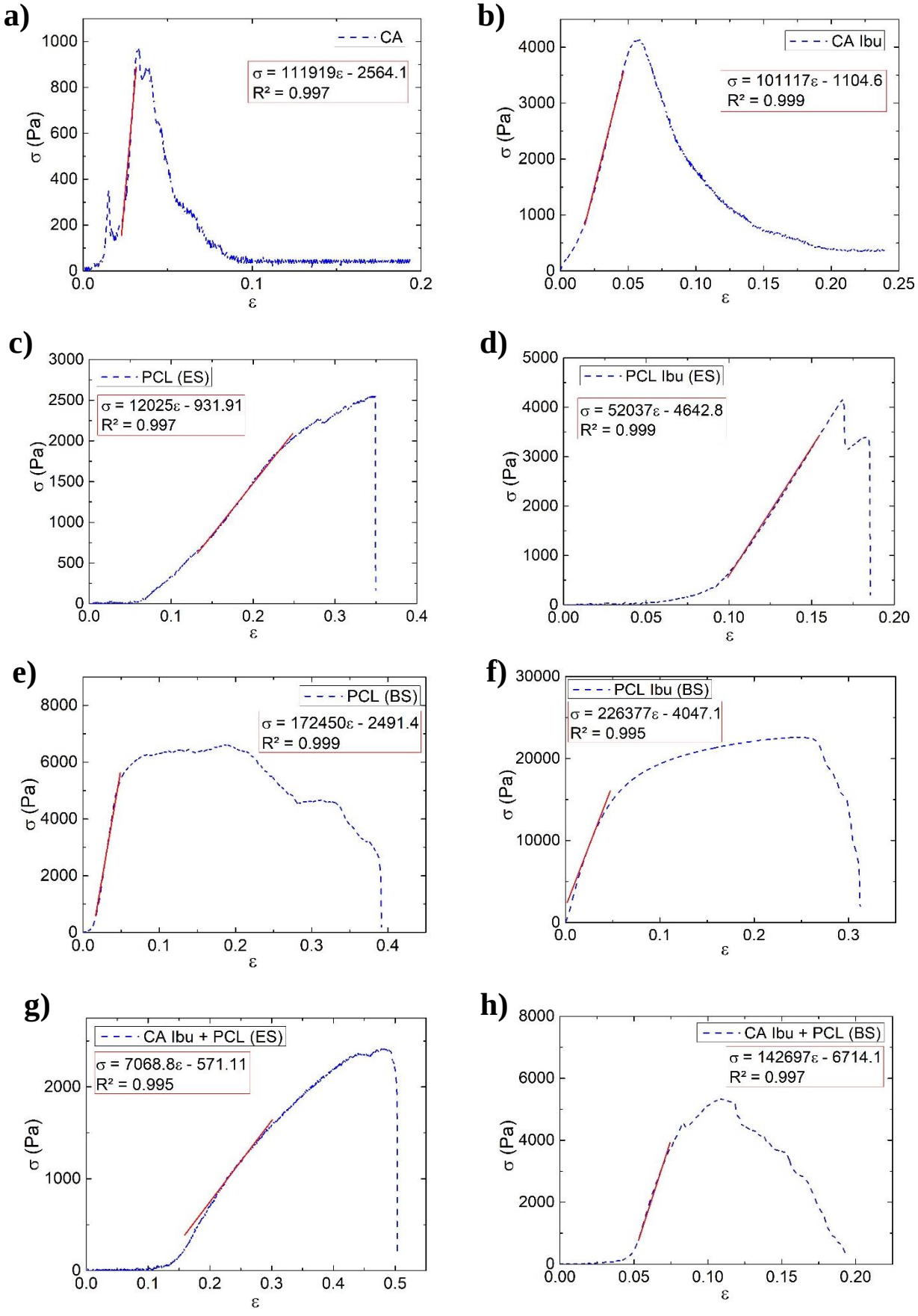

Figure 3.15 - Example of a stress-strain curves from each type of membrane a) CA, b) CA Ibu, c) PCL ES, d) PCL Ibu ES, e) PCL BS, f) PCL Ibu BS, g) CA Ibu + PCL (ES), h) CA Ibu + PCL (BS)

Figure 3.15 shows that the a) and b) membranes experience a small plastic deformation followed by a sudden drop in stress, indicating brittle fracture. In contrast to membranes e), f), and h), which show elastic deformation indicating ductile fracture. The c), d) and g) membranes, show possible behaviour curves for brittle materials, but the membranes stretch beyond 50% of their elongation, so it is considered ductile behaviour. These behaviours are related to the type of polymer and production technique used. PCL membranes are naturally more elastic than CA membranes, but when produced by BS, this characteristic becomes more apparent.

The differences in force can also be attributed to different membrane production techniques, environmental conditions, or even variations in thickness, causing membranes to rip sooner with less force. The Table 3.3 presents the average values of thickness, Young's modulus, yield strength and ultimate strength of the membranes used in the tests.

Table 3.3 - Average thickness (mm), Young's modulus (MPa), yield strength (Pa) and ultimate strength (Pa) of the tested membranes

Membrane	Thickness (mm)	Young's modulus (MPa)	Yield strength (Pa)	Ultimate strength (Pa)
CA	0.039 ± 0.015	0.107 ± 0.008	858.3 ± 153.2	
CA Ibu	0.053 ± 0.004	0.155 ± 0.049	5422.2 ± 1614.6	
PCL (ES)	0.027 ± 0.007	0.012 ± 0.001	2400 ± 212.1	
PCL Ibu (ES)	0.067 ± 0.010	0.051 ± 0.016	3855.6 ± 2299.2	
PCL (BS)	0.089 ± 0.021	0.248 ± 0.129	21938.9 ± 14064.4	28061.1 ± 18812.2
PCL Ibu (BS)	0.113 ± 0.023	0.208 ± 0.112	13825.3 ± 7328.4	18500 ± 10326.6
CA Ibu + PCL (ES)	0.019 ± 0.002	0.008 ± 0.001	1841.7 ± 836.7	
CA Ibu + PCL (BS)	0.045 ± 0.006	0.288 ± 0.205	5208.5 ± 907.2	7516.7 ± 3087.7

The tensile tests were the last ones done in this study, so the available membranes had very thin thicknesses compared to the ones found in the literature, resulting in less accurate results. Despite this, it is possible to compare the results obtained by the various membranes.

PCL made by BS demonstrated excellent elasticity and strength. PCL is already known for its high mechanical strength, however CA has relatively poor mechanical properties. As a result, the CA-PCL system can overcome CA's poor mechanical properties to achieve significant strength[33]. Blending CA with PCL increased tensile strength compared to CA, achieving a reasonable balance of flexibility and hardness, as shown in Table 3.3.

3.4.4 Peeling-off tests

To test the adhesion of the membrane to the surface of the SS substrate, the substrates were fixed into a uniaxial traction machine, with one side held by a clamp and a piece of tape, that was placed over the membrane, also held by a clamp. All membranes were electrospun onto the substrates, and some had the added feature of an electrosprayed layer of CHI between the substrate and the membrane to evaluate its effect on adhesion. The schematic of the setup used for the tests is shown in Figure 3.16 [34].

The SS substrates were tested with a speed of 5 mm/min and increasing force up to 5 N pulling the tape. The results are showed in Table 3.4.

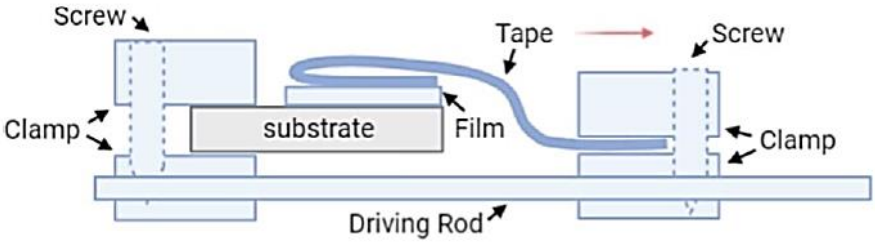

Figure 3.16 - Schematic of the setup used for adhesion tests[34].

Table 3.4 - Average force of the adhesion tests for various substrates

SS Substrates	Average Force (N)	
	without CHI	with CHI
CA	0.15 ± 0.02	0.21 ± 0.03
CA Ibu	0.20 ± 0.03	0.22 ± 0.03
PCL	0.20 ± 0.03	0.30 ± 0.02
PCL Ibu	0.22 ± 0.02	0.27 ± 0.03
CA + PCL	0.21 ± 0.04	0.46 ± 0.06
CA Ibu + PCL Ibu	0.22 ± 0.05	0.74 ± 0.05

Comparing the results in the Table 3.4, it is possible to confirm that CHI increases membrane adhesion to the substrate, particularly in the CA+PCL mixtures. Because the polymers have opposite charges (CA is negatively charged and CHI layer is positively charged), electrostatic forces will contribute to this adhesion[26].

Following the peeling-off tests, it was possible to conclude, in a qualitative evaluation, that the substrates with CHI (Figure 3.17 a)) continued to have membranes attached, while the substrates without CHI (Figure 3.17 b)) remained practically without traces of the membranes, demonstrating the influence of the CHI in adhesion once more.

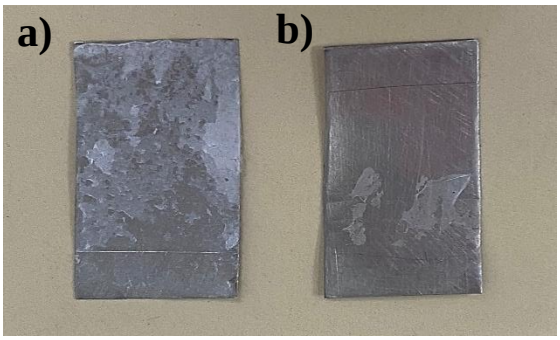

Figure 3.17 - SS substrates after peeling-off test a) with CHI, b) without CHI

4

CONCLUSIONS AND FUTURE PERSPECTIVES

The purpose of this research was to investigate the application of polymeric coatings on stainless-steel (SS) surfaces, as well as drug incorporation and release to prevent the formation of biofilms and the failure of medical implants.

Cellulose acetate (CA) and polycaprolactone (PCL) were the chosen polymers, because of their biocompatibility, drug retention capacity, and use in previous studies with positive results. To produce fibre membranes and deposit on SS substrates, solutions of CA without or with 1 mg of ibuprofen (Ibu) were produced by the electrospinning (ES) technique, while solutions of PCL without or with 1 mg of Ibu were produced by ES or blow-spinning (BS) techniques. The SS substrates were cleaned and mechanically treated, to improve the adhesion of the membranes to the substrates.

The diameters of the electrospun fibres were measured from SEM images using the ImageJ® program. CA fibres without Ibu had an average diameter of 439 nm, while CA fibres with Ibu had an average diameter of 921 nm. PCL fibres without Ibu had an average diameter of 312 nm, while those with Ibu had a diameter of 726 nm. CA+PCL fibres without Ibu had an average diameter of 446 nm, while those with Ibu had an average diameter of 703 nm. This diameters difference shows a tendency to form larger fibres when Ibu is added, which appears to be the result of fibre fusion. However, other parameters such as Ibu agglomeration and change in viscosity cannot be excluded.

Raman spectroscopy was used to confirm drug incorporation in the CA and PCL membranes. Some of the most distinctive peaks of the Ibu compounds were identified through analysis of their individual spectra. Thus, by comparing the spectra obtained from the CA and PCL membranes with and without Ibu, the presence of Ibu in its composition was identified.

The drug release tests were carried out in both simulated body fluid (SBF) solution and water. They were carried out by immersing membrane pieces containing Ibu in SBF or water, with a volume to avoid oversaturation of the Ibu during release. For 7 days, the absorption spectra of SBF or water mediums with Ibu concentrations were measured at various intervals. The absorbance values were compared to those of a calibration curve that was obtained by diluting a solution of SBF with 20 mg/L concentration of ibuprofen from 0 mg/L to 20 mg/L in 1 mg/L intervals. Water followed the same procedure.

The drug release tests results show that Ibu was successfully released, but with different behaviours depending on which membrane it was encapsulated and its producing technique. When comparing PCL Ibu (ES) to PCL Ibu (BS), or CA Ibu + PCL (ES) to CA Ibu + PCL (BS), it is verified that PCL dissolution is faster in BS membranes due to porosities, whereas in ES it takes longer to dissolve PCL and then release the drug. It was also determined that the PCL Ibu membrane releases drug more easily than the CA Ibu membrane.

However, the obtained values of Ibu released were inaccurate due to the non-uniform distribution of Ibu in the membrane. To obtain more precise results, it would be necessary, for example, to increase the number

of samples or to use a more specific technique for Ibu quantification, as the absorption of SBF salts or polymers can hide the Ibu absorption values.

The degradation tests performed on the fibres revealed that mass loss remained relatively low through the process. CA mass loss stabilises between 5% and 10% after 10 days, and PCL mass loss stabilises at 30% after 13 days. Sweeling tests were also performed to supplement this information. The swelling ratio for PCL was low throughout the process, peaking at 213% after 6 days and then stabilising between 115% and 135%, as expected given that PCL is hydrophobic, which means it is insoluble in any type of aqueous solution. As a result, the high drug delivery in PCL Ibu membranes can be explained by swelling and mass losses. In the case of CA membranes, mass loss is low while swelling is very high, which is ideal for drug carriers. However, when needed drug retention PCL can be a possible choice.

Mechanical performance of membranes produced with or without Ibu was expected, with a Young's modulus ranging from 0.008 to 0.288 MPa. The membranes containing Ibu had a higher Young's modulus than those without. Membrane production techniques, environmental conditions, and even variations in thickness can cause membranes to tear faster and with less force. It was also observed that PCL membranes were naturally more elastic than CA membranes, but when produced by BS, this characteristic is even more evident.

A layer of chitosan (CHI) was electrosprayed for some substrates before the CA or PCL membranes with the objective of improving adhesion. Due to the conductive nature of the SS substrates, no changes to the electrospinning assembly were required, resulting in the same parameters used to produce the membranes. Membrane adhesion testing to substrates revealed that the addition of the CHI layer increased peel-off force, resulting in a force range of 0.15-0.22 N without CHI and 0.21-0.74 N with CHI.

In conclusion, the thesis's goals were achieved, however, there is still much to investigate about this subject. Some of the processes used could be optimised, as well as changes and/or additions that could solidify this coating as a method of combating biofilm formation.

In future, some topics worth researching or pursue include:

i. Prevent fibre fusion by reducing the diameter of the fibres, using a more controlled environment, or improving the ES parameters.
ii. Experiment deposition of other polymers using the BS technique and standardise the production parameters.
iii. Create coatings by adapting polymers and their producing techniques to the needs of the drug delivery system (higher release initially or more continuous release over time).
iv. Perform more tests to have better statistics and control the amount of drug release.
v. Use a CHI layer to improve membrane adherence in SS substrates.
vi. Perform proliferation tests to understand the extent to which the biofilm is formed or controlled by the application of the drug and films to the metal substrates.

5 REFERENCES

[1] Romaní, A. M., Fund, K., Artigas, J., Schwartz, T., Sabater, S., & Obst, U. "Relevance of polymeric matrix enzymes during biofilm formation". *Microbial Ecology*, *56*(3), pp. 427–436, 2008. https://doi.org/10.1007/s00248-007-9361-8

[2] Veerachamy, S., Yarlagadda, T., Manivasagam, G., & Yarlagadda, P. K. "Bacterial adherence and biofilm formation on medical implants: A review". *Proceedings of the Institution of Mechanical Engineers, Part H: Journal of Engineering in Medicine*, *228*(10), pp. 1083–1099, 2014. https://doi.org/10.1177/0954411914556137

[3] Ko, S., Lee, J., Nam, J. "Effectiveness of orthopedic implant removal surgery in patients with no implant-related symptoms after fracture union of isolated lower extremity shaft fractures: patient-centered evaluation". *Archives of Orthopaedic and Trauma Surgery*, 2021. https://doi:10.1007/s00402-021-03993-y

[4] Maunders, E., & Welch, M. "Matrix exopolysaccharides; the sticky side of biofilm formation". *FEMS Microbiology Letters*, *364*(13), pp. 1–10, 2017. https://doi.org/10.1093/femsle/fnx120

[5] Galante, J. O., Lemons, J., Spector, M., Wilson, P. D., & Wright, T. M. The biologic effects of implant materials. *Journal of Orthopaedic Research*, *9*(5), pp. 760–775, 1991 https://doi.org/10.1002/jor.1100090516

[6] Mahmoudi Hashemi, P., Borhani, E., & Nourbakhsh, M. S. "A review on nanostructured stainless-steel implants for biomedical application". *Nanomedicine Journal*, *3*(4), pp. 202–216, 2016. https://doi.org/10.22038/nmj.2016.7574

[7] Renz, N., Mudrovcic, S., Perka, C., & Trampuz, A. "Orthopedic implant-associated infections caused by Cutibacterium spp. – A remaining diagnostic challenge". *PLoS ONE*, *13*(8), 2018. https://doi.org/10.1371/journal.pone.0202639

[8] Liu, B., & Zheng, Y. F. "Effects of alloying elements (Mn, Co, Al, W, Sn, B, C and S) on biodegradability and in vitro biocompatibility of pure iron". *Acta Biomaterialia*, *7*(3), pp. 1407–1420, 2011. https://doi.org/10.1016/j.actbio.2010.11.001

[9] Pradilla, G., Thai, Q. A., Legnani, F. G., Clatterbuck, R. E., Gailloud, P., Murphy, K. P., & Tamargo, R. J. "Local delivery of ibuprofen via controlled-release polymers prevents angiographic vasospasm in a monkey model of subarachnoid hemorrhage". *Neurosurgery*, *57*(1 SUPPL.), pp. 184–190, 2005. https://doi.org/10.1227/01.NEU.0000163604.52273.28

[10] Vatanpour V, Pasaoglu ME, Barzegar H, Teber OO, Kaya R, Bastug M, Khataee A, Koyuncu I. "Cellulose acetate in fabrication of polymeric membranes: A review". Chemosphere. 295:133914, 2022. doi: 10.1016/j.chemosphere.2022.133914.

[11] Liu, H., & Hsieh, Y. Lo. "Ultrafine fibrous cellulose membranes from electrospinning of cellulose acetate". *Journal of Polymer Science, Part B: Polymer Physics*, *40*(18), pp. 2119–2129, 2002. https://doi.org/10.1002/polb.10261

[12] Laurence Mckeen. "Renewable Resource and Biodegradable Polymers," in *The Effect of Sterilization on Plastics and Elastomers*, 4th ed., J. Bayliss, Ed. Chennai, India: Elsevier Inc., pp. 305–317, 2012.

[13] J. Drobnik, I. Krucinska, A. Komisarczyk, S. Sporny, A. Szczepanowska, and J. Ciosek. "Effects of electrospun scaffolds of di-O-butyrylchitin and poly-(ε-caprolactone) on wound healing," *Neuropept. Res.*, vol. 60, no. 3, pp. 162–171, 2017.

[14] Azevedo, V. V. C., Chaves, S. a, Bezerra, D. C., Fook, M. V. L., & Costa, a C. F. M. "Quitina e Quitosana: aplicações como biomateriais". *Revista Eletrônica de Materiais e Processos*, *2.3*, pp. 27–34, 2007.

[15] M. R. Leedy, H. J. Martin, P. A. Norowski, J. A. Jennings, W. O. Haggard, and J. D. Bumgardner."Use of Chitosan as a Bioactive Implant Coating for Bone-Implant Applications," *Adv. Polym. Sci.*, vol. 244, 2011.

[16] Goyanes SN, D'Accorso NB. "Industrial applications of renewable biomass products: Past, present and future". *Ind Appl Renew Biomass Prod Past, Present Futur*. 2017: 1-332, 2019. doi:10.1007/978-3-319-61288-1

[17] Rainsford, K. D. "Ibuprofen: Pharmacology, efficacy, and safety". *Inflammopharmacology*, *17*(6), pp. 275–342, 2009. https://doi.org/10.1007/s10787-009-0016-x

[18] Ali Mohammadpoor, S., Akbari, S., Sadrjahani, M., & Nourpanah, P. "Fabrication of electrospun ibuprofen-loaded poly(vinyl alcohol)/hyper-branched poly(ethylenimine) fibers and their release behaviors". *Journal of Biomaterials Science, Polymer Edition*, *31*(2), pp. 261–275, 2020. https://doi.org/10.1080/09205063.2019.1685759

[19] Rahman, Mohammed Muzibur; Asiri, Abdullah M. "Nanofibre Research - Reaching New Heights || Electrospinning and Electrospraying Techniques for Designing Antimicrobial Polymeric Biocomposite Mats". 10.5772/61952(Chapter 5), 2016. doi:10.5772/63470

[20] Torres-Martinez, E. J., Cornejo Bravo, J. M., Serrano Medina, A., Pérez González, G. L., & Villarreal Gómez, L. J. "A Summary of Electrospun Nanofibers as Drug Delivery System: Drugs Loaded and Biopolymers Used as Matrices". *Current Drug Delivery*, *15*(10), pp. 1360–1374, 2018. https://doi.org/10.2174/1567201815666180723114326

[21] Czarnecka, K., Wojasiński, M., Ciach, T., & Sajkiewicz, P. "Solution blow spinning of polycaprolactone-rheological determination of spinnability and the effect of processing conditions on fiber diameter and alignment". *Materials*, *14*(6), 2021. https://doi.org/10.3390/ma14061463

[22] NanofibersLabs. Introductory tutorial for electrospinning. Available: https://www.nanofiberlabs.com/solutions/introductory-tutorial-for-electrospinning.html

[23] Zhang, T., Tian, H.,Yin, X., Li, Z., Zhang, X., Yang, J., Zhu, L. "Solution Blow Spinning of Polylactic Acid to Prepare Fibrous Oil Adsorbents Through Morphology Optimization with Response Surface Methodology". *Journal of Polymers and the Environment*, 2020. https://doi.org/10.1007/s10924-019-01617-6

[24] Shi, Y., Wei, Z., Zhao, H., Liu, T., Dong, A., & Zhang, J. "Electrospinning of ibuprofen-loaded composite nanofibers for improving the performances of transdermal patches". *Journal of Nanoscience and Nanotechnology*, *13*(6), pp. 3855–3863, 2013. ://doi.org/10.1166/jnn.2013.7157

[25] Zhu, Y., Liu, W., & Ngai, T. "Polymer coatings on magnesium-based implants for orthopedic applications". *Journal of Polymer Science*, *60*(1), pp. 32–51, 2022. https://doi.org/10.1002/pol.20210578

[26] Faria, J., Dionísio, B., Soares, Í., Baptista, A. C., Marques, A., Gonçalves, L., Bettencourt, A., Baleizão, C., & Ferreira, I. "Cellulose acetate fibres loaded with daptomycin for metal implant coatings". *Carbohydrate Polymers*, *276*, 2022. https://doi.org/10.1016/j.carbpol.2021.118733

[27] Freire, João. (2021). "Anti-bacterial surface protection for prostheses". Dissertação de Mestrado, Faculdade de Ciência e Engenharia, Universidade Nova de Lisboa.

[28] Cüneyt Tas, A. "Synthesis of biomimetic Ca-hydroxyapatite powders at 37°C in synthetic body fluids". *Biomaterials*, *21*(14), pp. 1429–1438, 2000. https://doi.org/10.1016/S0142-9612(00)00019-3

[29] Brito, Miguel. "Desenvolvimento de membranas funcionalizadas para libertação controlada de fármaco em aplicações tópicas". 2020. Dissertação de Mestrado, Faculdade de Ciência e Engenharia, Universidade Nova de Lisboa.

[30] Dias, J. R., Sousa, A., Augusto, A., Bártolo, P. J., & Granja, P. L. "Electrospun Polycaprolactone (PCL) Degradation: An In Vitro and In Vivo Study". *Polymers*, *14*(16), pp. 1–15, 2022. https://doi.org/10.3390/polym14163397

[31] M. Bartnikowski, T. R. Dargaville, and D. W. Hutmacher, "Progress in Polymer Science Degradation mechanisms of polycaprolactone in the context of chemistry, geometry and environment," vol. 96, pp. 1–20, 2019.

[32] Mark Karadsheh. Material strength: stress vs strain curve. Available: https://www.orthobullets.com/basic-science/9062/material-properties

[33] Liao, N., Unnithan, A. R., Joshi, M. K., Tiwari, A. P., Hong, S. T., Park, C. H., & Kim, C. S. "Electrospun bioactive poly (e{open}-caprolactone)-cellulose acetate-dextran antibacterial composite mats for wound dressing applications". *Colloids and Surfaces A: Physicochemical and Engineering Aspects*, *469*, pp. 194–201, 2015. https://doi.org/10.1016/j.colsurfa.2015.01.022

[34] Soares Í. "Multifunctional coatings of polymeric films for biofilm-mediated infections". 2020. Dissertação de Mestrado, Faculdade de Ciência e Engenharia, Universidade Nova de Lisboa.

6

ANNEXES

6.1 Annex A

Table A.1 shows the electrospinning parameters used to produce cellulose acetate membranes and for the deposition of the cellulose acetate solutions with and without ibuprofen, onto the substrates.

Table A.1 - Electrospinning parameters for CA solution

	CA solution	
Parameters	**With ibuprofen**	**Without ibuprofen**
Voltage	18 kV	20 kV
Flow Rate	0.2 mL/h	
Needle	25G	
Temperature	20 – 28ºC	
Humidity	30 – 50%	
Distance from target	15 cm	

6.2 Annex B

Table B.1 shows the electrospinning parameters used to produce polycaprolactone membranes and for the deposition of the polycaprolactone solutions with and without ibuprofen, onto the substrates.

Table B.1 - Electrospinning parameters for PCL solution

	PCL solution	
Parameters	**With ibuprofen**	**Without ibuprofen**
Voltage	18 kV	
Flow Rate	0.5 mL/h	
Needle	25G	
Temperature	20 – 28ºC	
Humidity	30 – 50%	
Distance from target	15 cm	

6.3 Annex C

Table C.1 shows the electrospray parameters used for the deposition of the chitosan layer on stainless-steel.

Table C.1 - Electrospray parameters for CHI solution

Parameters	Values
Voltage	20 kV
Flow Rate	0.2 mL/h
Needle	25G
Temperature	20 – 28ºC
Humidity	30 – 50%
Distance from target	15 cm

6.4 Annex D

In Table D.1 the steps for the cleaning and treatment of the stainless-steel substrates are described in order. The mechanical treatment was done manually consisting of 100 passes horizontally, vertically and in a circular motion with sandpaper.

Table D.1 - Stainless-steel cleaning and treatment steps[27]

Steps	Cleaning and treatment description of stainless steel	Duration
1	Cut into 1 by 1.5 cm	NA
2	Ultrapure water ultrasound bath	5 min
3	Acetone ultrasound bath	5 min
4	Oven 300°C	10 min
5	Acetone ultrasound bath	10 min
6	Ultrapure water ultrasound bath	10 min
7	Submerge in sodium hydroxide (0.75 M)	4 min
8	Mechanical treatment	NA
9	Ultrapure water ultrasound bath	15 min
10	Ethanol ultrasound bath	15 min
11	Toluene ultrasound bath	15 min
12	Vacuum -1 Bar at 70°C	90 min

6.5 Annex E

Table E.1 shows the components used to make the simulated body fluid solution, in order of addition. The reagents are added one by one, after total dissolution, in 700 mL of distilled water. After adding the 9th reagent, the solution was warmed from room temperature to 37ºC. Then, hydrochloric acid should be added to lower the pH and, finally, add water to cover 1L of solution.

Table E.1 – SBF solution components[28]

Order	Component	Formula	Mass (g)
1	Sodium chloride (Sigma-Aldrich, Germany)	NaCl	6.547
2	Sodium carbonate (PanReacAppliChem, Germany)	$NaHCO_3$	2.268
3	Potassium chloride (Scharlau, Spain)	KCl	0.373
4	Sodium phosphate dibasic dihydrate (FLuka Analytical)	$Na_2HPO_4{\cdot}H2O$	0.178
5	Magnesium chloride hexahydrate (PanReacAppliChem, Germany)	$MgCl_2{\cdot}6H_2O$	0.305
6	Hydrochloric acid (1 M)	HCl	15 mL
7	Calcium chloride dihydrate (Sigma-Aldrich, Germany)	$CaCl_2{\cdot}2H_2O$	0.368
8	Sodium sulphate (Sigma-Aldrich, Germany)	Na_2SO_4	0.071
9	Tris(hydromethyl)aminomethane (Sigma-Aldrich, USA)	$(CH_2OH)_3CNH_2$	6.057
10	Hydrochloric acid (1 M)	HCl	“tritate” up to pH 7.4 at 37ºC

6.6 Annex F

Table F.1 contains the volumes of SBF solutions without ibuprofen and with 20 mg/L ibuprofen concentration, used to make the several dilutions for 10 mL of total solution. These dilutions were made to set up the ibuprofen calibration curve in SBF.

Table F.1 - Dilutions of SBF solution with ibuprofen for calibration curve

Concentration (mg/L)	SBF solution (mL)	SBF solution with ibuprofen (mL)
0	10	0
1	9.5	0.5
2	9	1
3	8.5	1.5
4	8	2
5	7.5	2.5
6	7	3
7	6.5	3.5
8	6	4
9	5.5	4.5
10	5	5
11	4.5	5.5
12	4	6
13	3.5	6.5
14	3	7
15	2.5	7.5
16	2	8
17	1.5	8.5
18	1	9
19	0.5	9.5
20	0	10

6.7 Annex G

Figure G.1 shows the absorbance spectra of the dilutions of SBF solution with ibuprofen, that were used to make the calibration curve.

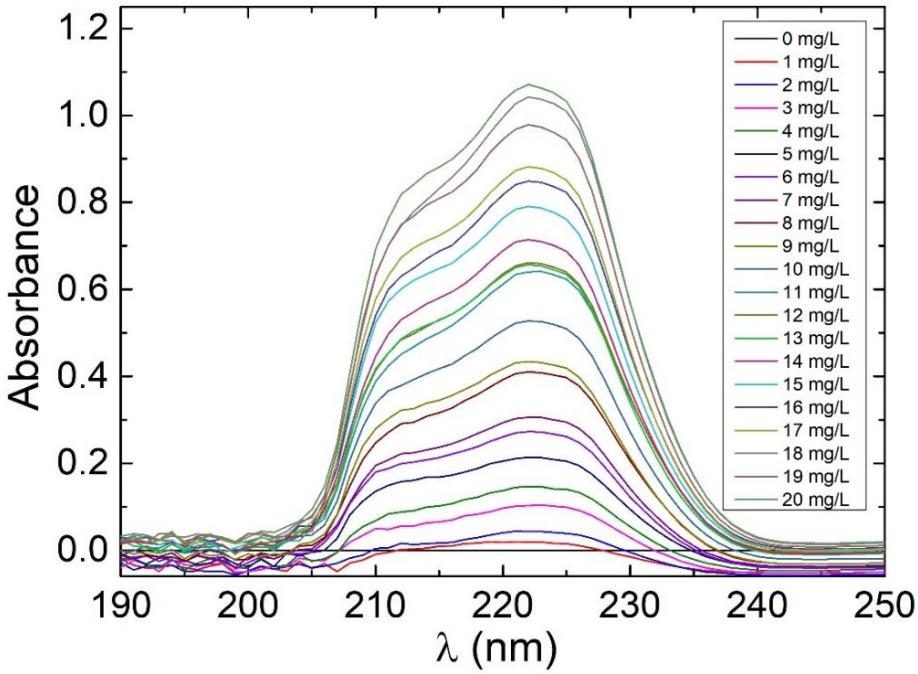

Figure G.1 - Absorbance spectra for the different ibuprofen concentrations in SBF, used for the calibration curve

6.8 Annex H

Figure H.1, Figure H.2, Figure H.3, Figure H.4, Figure H.5, Figure H.6 and Figure H.7 show the absorbance spectra of the cumulative ibuprofen release from all membranes in SBF. Used together with the calibration curve to determine the concentration of ibuprofen in the different solution on the represented intervals.

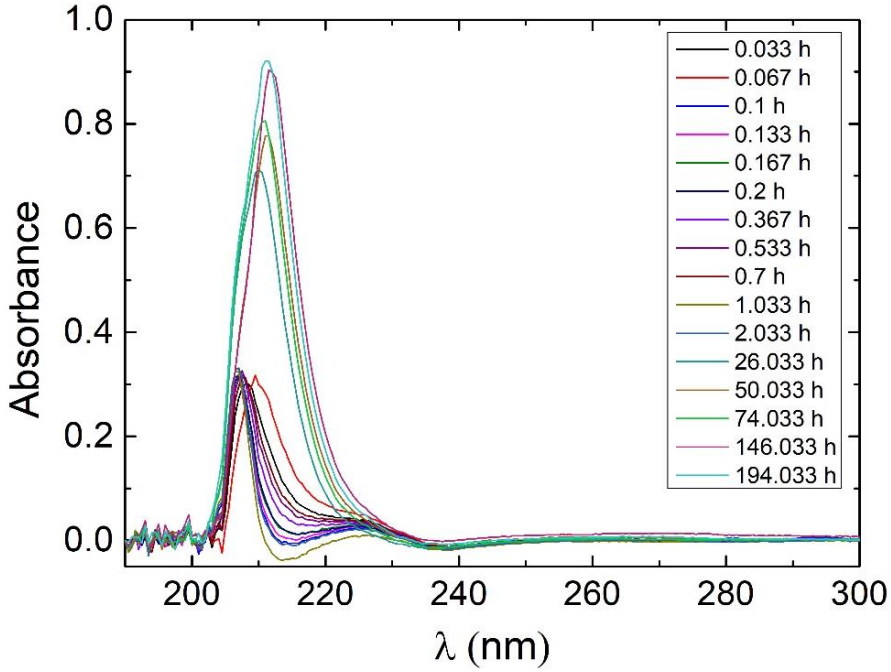

Figure H.1 - Absorbance spectra for CA Ibu membrane in SBF

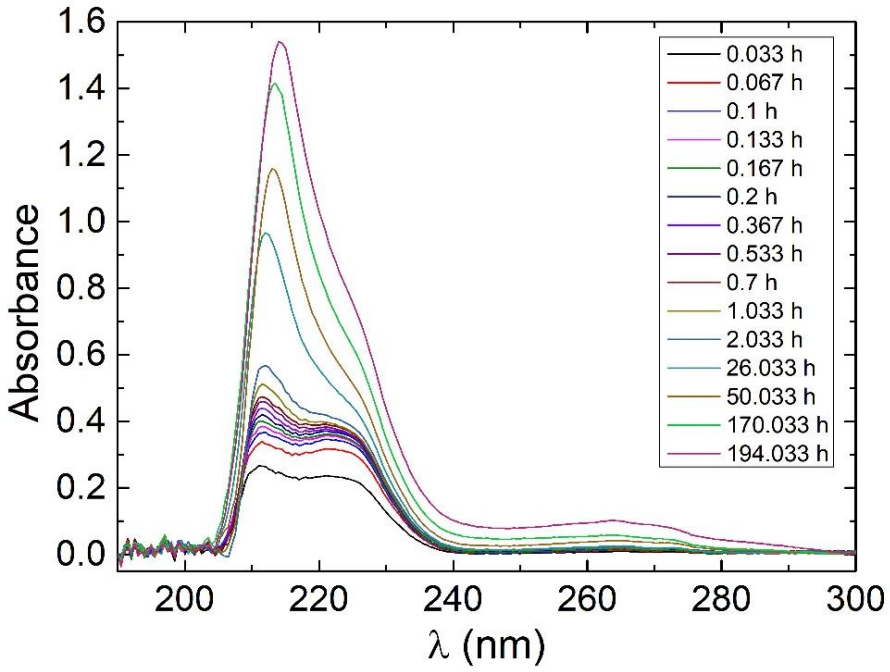

Figure H.2 - Absorbance spectra for PCL Ibu (ES) membrane in SBF

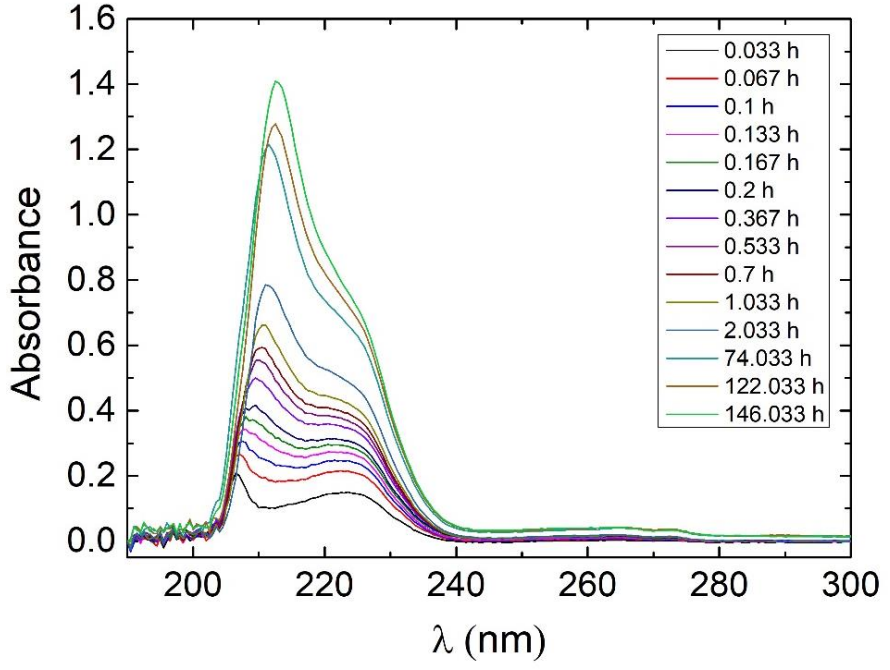

Figure H.3 – Absorbance spectra for PCL Ibu (BS) membrane in SBF

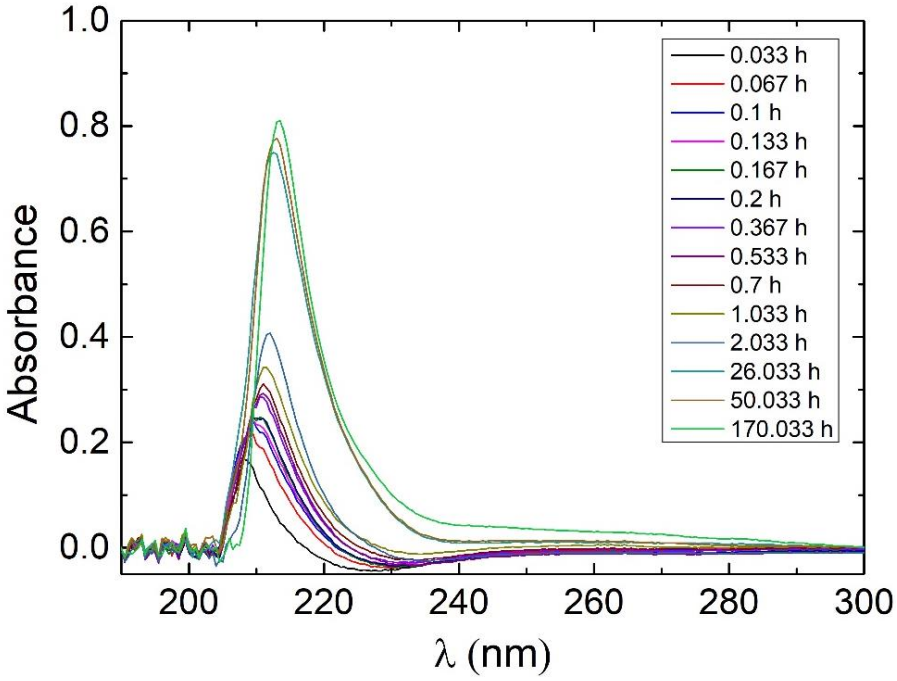

Figure H.4 - Absorbance spectra for CA + PCL Ibu (ES) membrane in SBF

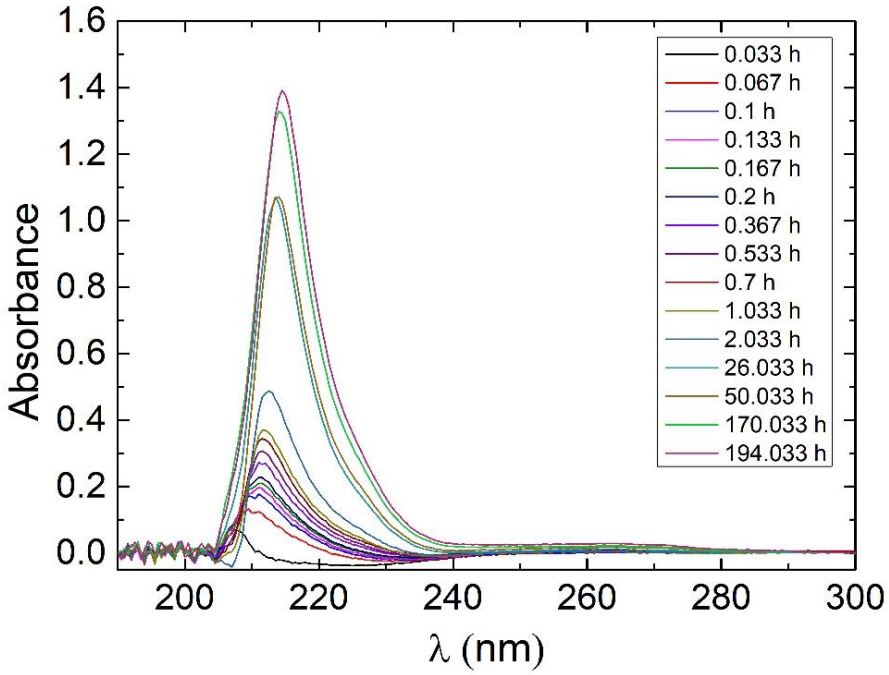

Figure H.5 - Absorbance spectra for CA + PCL Ibu (BS) membrane in SBF

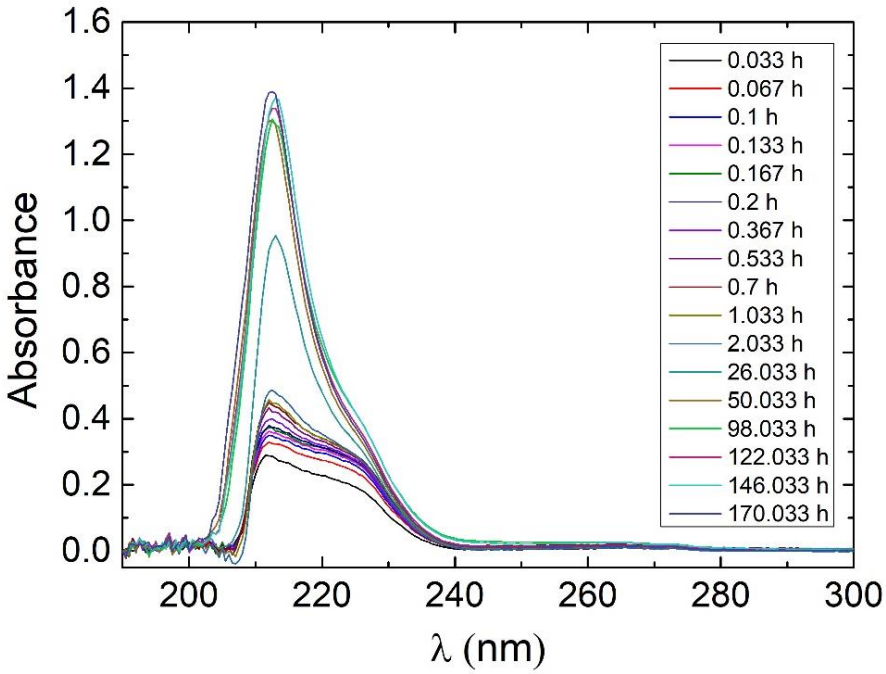

Figure H.6 - Absorbance spectra for CA Ibu + PCL (ES) membrane in SBF

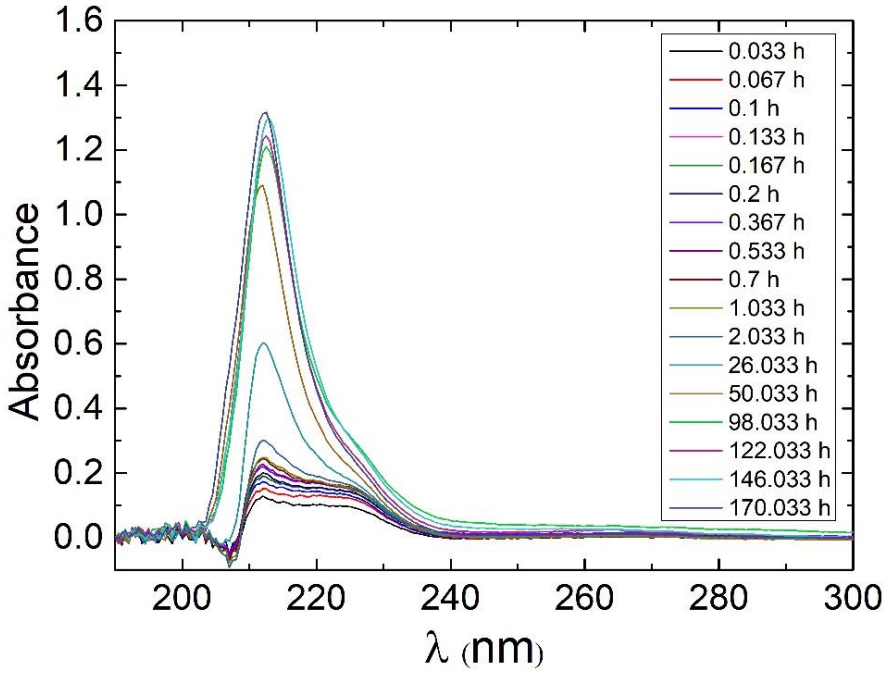

Figure H.7 – Absorbance spectra for CA Ibu + PCL Ibu (ES) membrane in SBF

Figure H.8, Figure H.9, Figure H.10, and Figure H.11 show the absorbance spectra of the cumulative ibuprofen release from all membranes in water. Used together with the calibration curve to determine the concentration of ibuprofen in the different solution on the represented intervals.

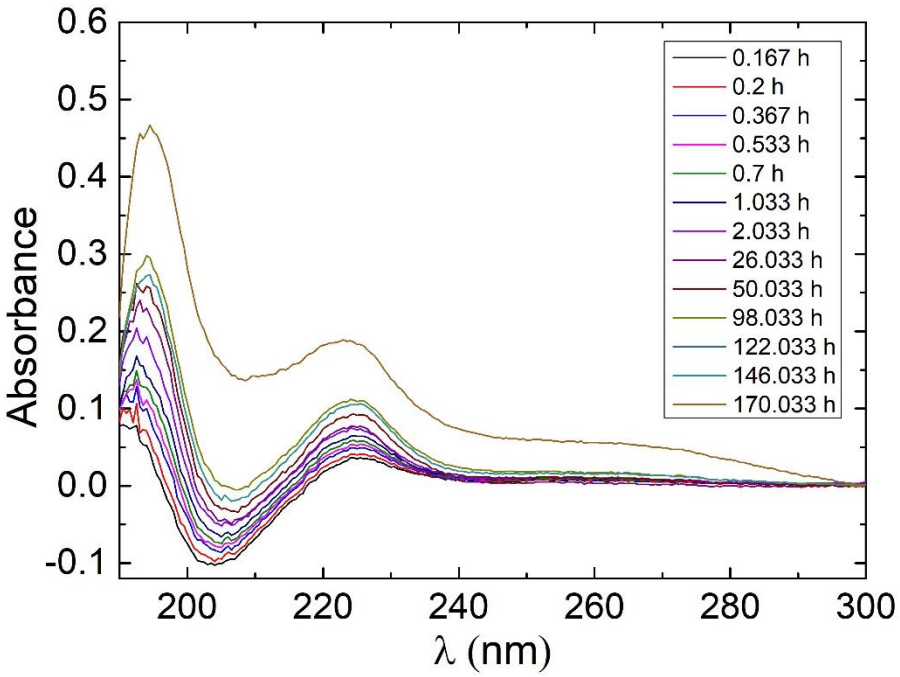

Figure H.8 - Absorbance spectra for CA Ibu membrane in water

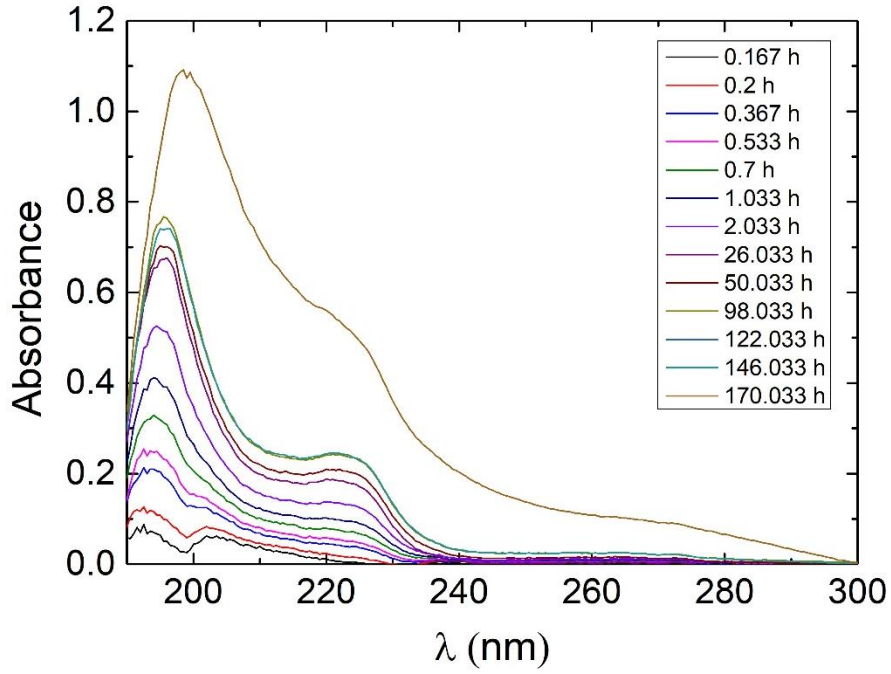

Figure H.9 - Absorbance spectra for PCL Ibu (ES) membrane in water

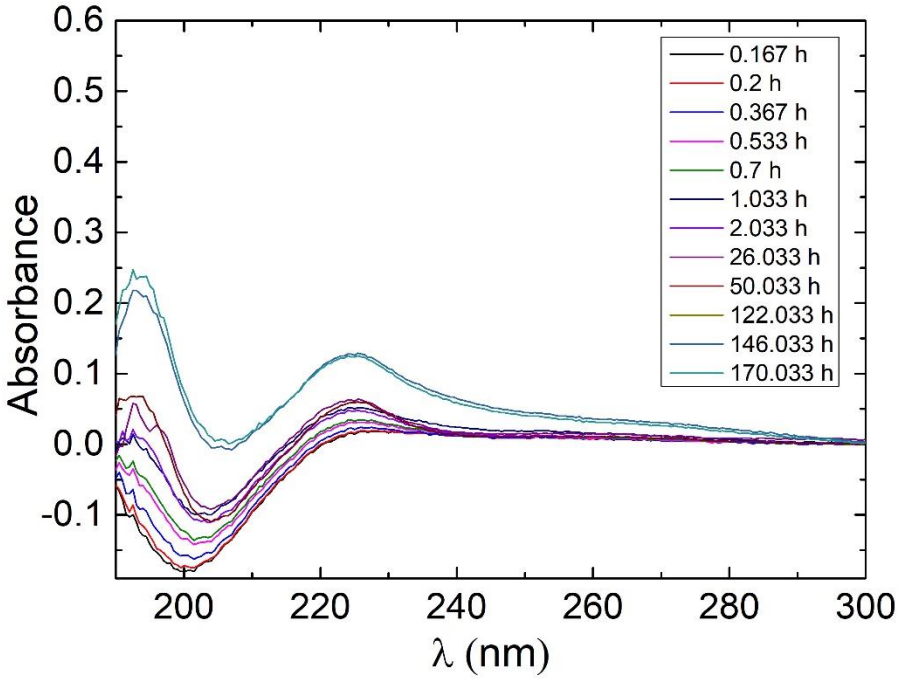

Figure H.10 - Absorbance spectra for CA Ibu + PCL (ES) membrane in water

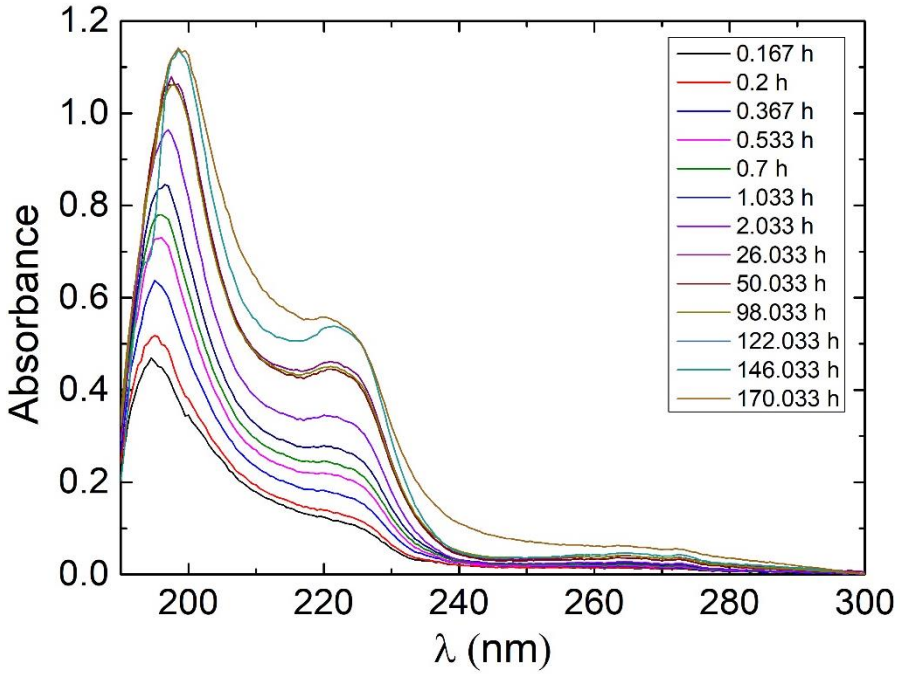

Figure H.11 - Absorbance spectra for CA + PCL Ibu (ES) membrane in water

2022

CATARINA PAULINO CIDADE DO CARMO

CONTROLLED DRUG DELIVERY FOR SURFACE PROTECTION OF PROSTHESES

NOVA SCHOOL OF SCIENCE & TECHNOLOGY